Chemical fixation of atmospheric CO_2 in tricopper(ii)-carbonato complexes with tetradentate *N*-donor ligands: reactive intermediates, probable mechanism, catalytic and magneto-structural studies

Narayan Ch. Jana,[a,b] Yu-Chen Sun,[c] Radovan Herchel,[d] Rakhi Nandy,[e] Paula Brandão,[f] Bidraha Bagh,[b] Xin-Yi Wang,[c] Anangamohan Panja[a,e*]

[a]*Department of Chemistry, Panskura Banamali College, Panskura RS, WB 721152, India. E-mail: ampanja@yahoo.co.in*

[b]*School of Chemical Sciences, National Institute of Science Education and Research (NISER), P.O. - Bhimpur-Padanpur, Jatni – 752050, Dist. -Khurda, Odisha, India*

[c]*State Key Laboratory of Coordination Chemistry, Collaborative Innovation Center of Advanced Microstructures, School of Chemistry and Chemical Engineering, Nanjing University, Nanjing, 210023, China. E-mail: wangxy66@nju.edu.cn*

[d]*Department of Inorganic Chemistry, Faculty of Science, Palacký University, 17. listopadu 12, 77146 Olomouc, Czech Republic*

[e]*Department of Chemistry, Gokhale Memorial Girls' College, 1/1 Harish Mukherjee Road, Kolkata 700020, India*

[f]*Department of Chemistry, CICECO-Aveiro Institute of Materials, University of Aveiro, 3810-193 Aveiro, Portugal*

Table of Contents

NMR Data of the Ligands

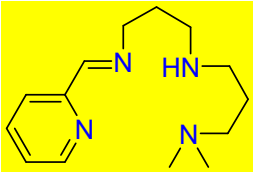

L^1: ^{1}H NMR (700 MHz, $CDCl_3$) δ 8.57 (s, 1H), 7.68 – 7.58 (m, 1H), 7.44 – 6.93 (m, 2H), 4.04 (d, *J* = 5.5 Hz, 1H), 3.27 (d, *J* = 11.1 Hz, 1H), 3.14 (d, *J* = 13.3 Hz, 1H), 2.75 (t, *J* = 13.0 Hz, 1H), 2.41 – 2.14 (m, 4H), 2.10 – 2.05 (m, 6H), 2.02 – 1.93 (m, 2H), 1.87 (dd, *J* = 12.2, 4.2 Hz, 1H), 1.66 – 1.42 (m, 3H). ^{13}C NMR (176 MHz, $CDCl_3$) δ 160.20 (s), 149.85 (s), 136.69 (s), 123.10 (s), 122.73 (s), 81.85 (s), 77.36 (s), 77.25 (d, *J* = 32.0 Hz), 76.98 (s), 57.79 (s), 52.19 (s), 51.83 (s), 45.33 (d, *J* = 9.8 Hz), 26.98 (s), 24.59 (s).

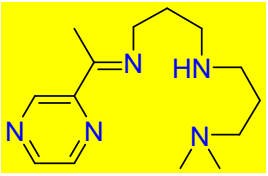

L^2: ^{1}H NMR (700 MHz, $CDCl_3$) δ 9.27 (d, *J* = 1.4 Hz, 1H), 8.50 (dd, *J* = 12.0, 9.6 Hz, 2H), 3.58 (s, 2H), 2.76 (dd, *J* = 9.2, 6.8 Hz, 2H), 2.65 (dd, *J* = 9.2, 6.8 Hz, 2H), 2.30 (d, *J* = 1.9 Hz, 3H), 2.29 – 2.27 (m, 2H), 2.18 (d, *J* = 2.6 Hz, 6H), 1.95 – 1.91 (m, 2H), 1.68 – 1.61 (m, 3H). ^{13}C NMR (176 MHz, $CDCl_3$) δ 165.14 (s), 152.40 (s), 144.48 (s), 143.49 (s), 142.69 (s), 77.34 (s), 77.16 (s), 76.98 (s), 58.15 (s), 50.93 (s), 48.60 (s), 48.48 (s), 45.64 (s), 31.12 (s), 28.25 (s), 13.70 (s).

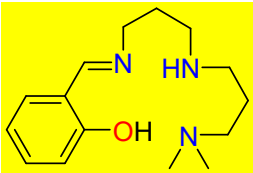

HL^3: ^{1}H NMR (400 MHz, $CDCl_3$) δ 8.32 (s, 1H), 7.32 – 7.13 (m, 3H), 6.99 – 6.76 (m, 3H), 3.62 (s, 2H), 2.66 (d, *J* = 20.6 Hz, 4H), 2.28 (s, 2H), 2.17 (s, 6H), 1.85 (s, 2H), 1.64 (dd, *J* = 13.4, 6.6 Hz, 3H), 1.23 (s, 1H). ^{13}C NMR (101 MHz, $CDCl_3$) δ 164.95 (s), 161.24 (s), 132.11 (s), 131.15 (s), 118.54 (s), 116.98 (s), 77.48 (s), 77.16 (s), 76.84 (s), 57.71 (d, *J* = 67.0 Hz), 57.28 – 57.09 (m), 48.53 (s), 47.48 (s), 45.49 (s), 31.05 (s), 27.73 (s).

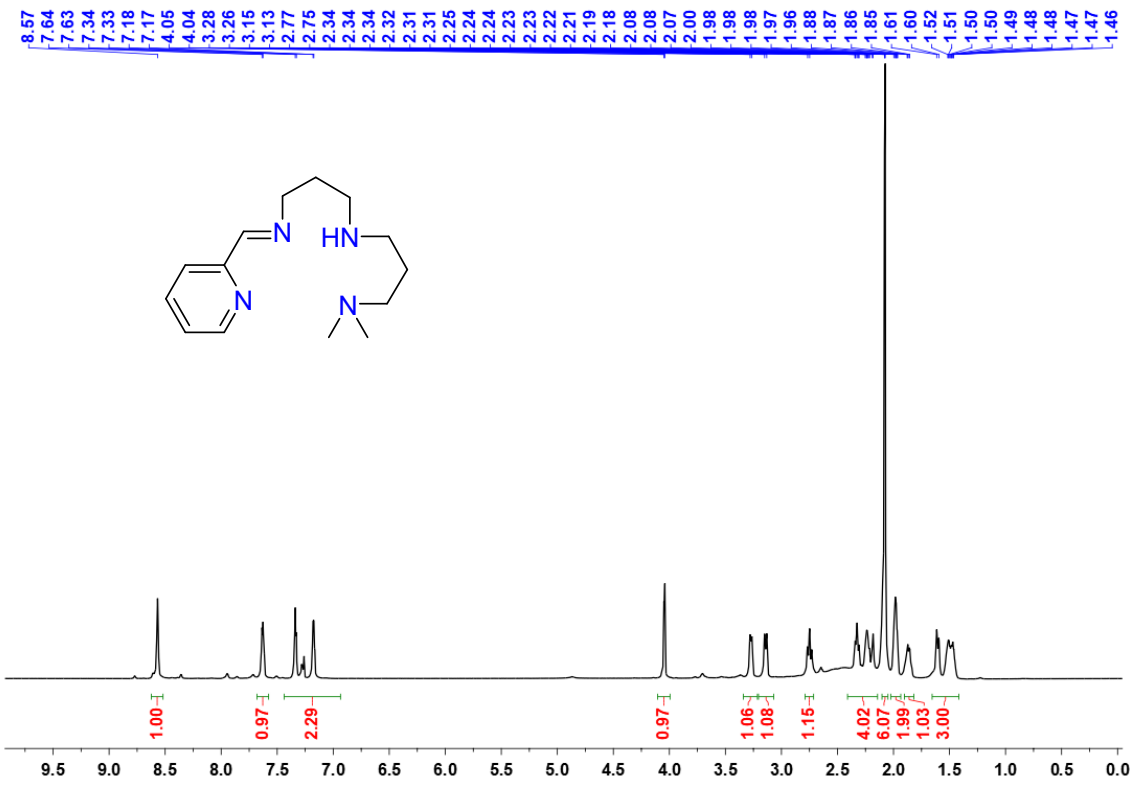

Fig. S1. ^{1}H NMR of (*E*)-N^1,N^1-dimethyl-N^3-(3-((pyridin-2-ylmethylene)amino)propyl)propane-1,3-diamine (**L^1**) in $CDCl_3$ at r.t.

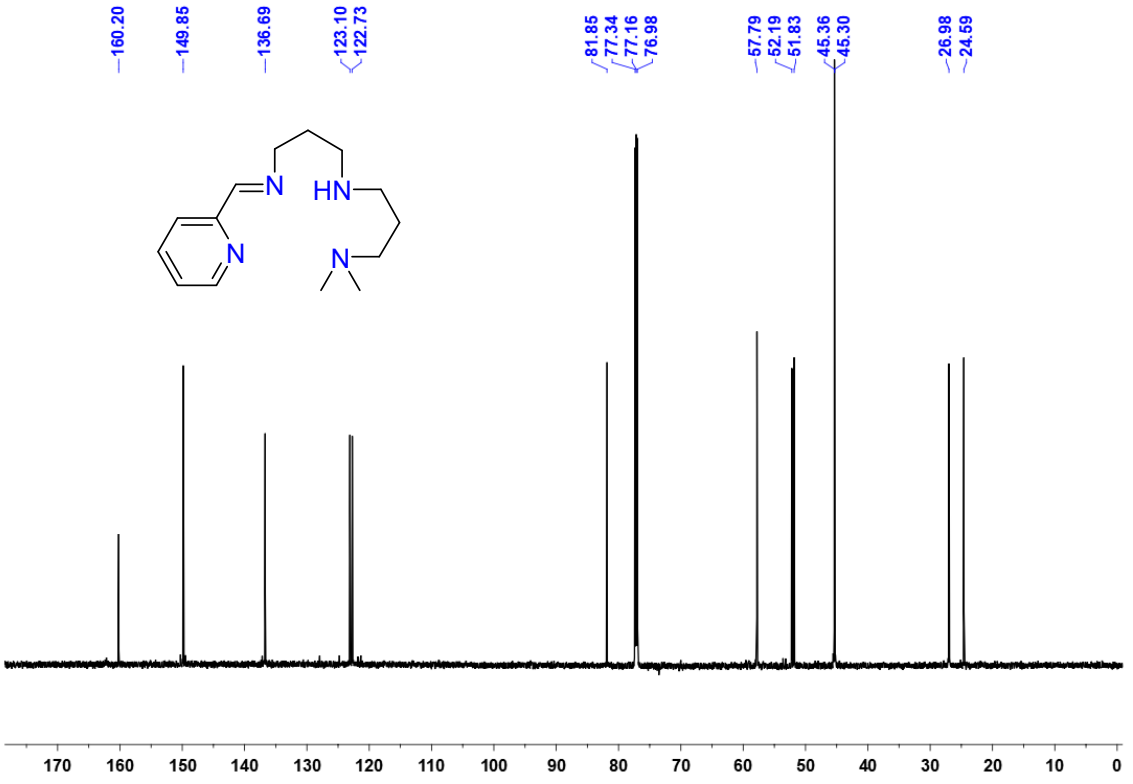

Fig. S2. ^{13}C NMR of (*E*)-N^1,N^1-dimethyl-N^3-(3-((pyridin-2-ylmethylene)amino)propyl)propane-1,3-diamine (**L^1**) in $CDCl_3$ at r.t.

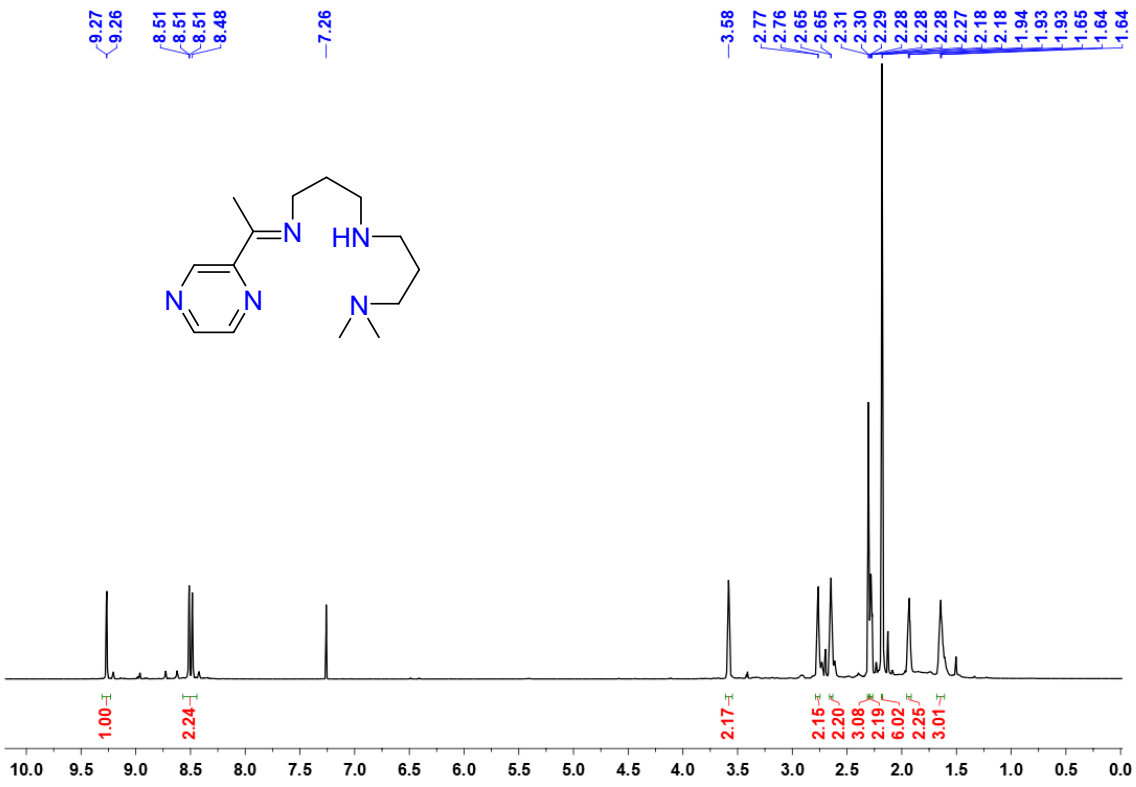

Fig. S3. ^{1}H NMR of (*E*)-N^1,N^1-dimethyl-N^3-(3-((1-(pyrazin-2-yl)ethylidene)amino)propyl)propane-1,3-diamine (**L²**) in $CDCl_3$ at r.t.

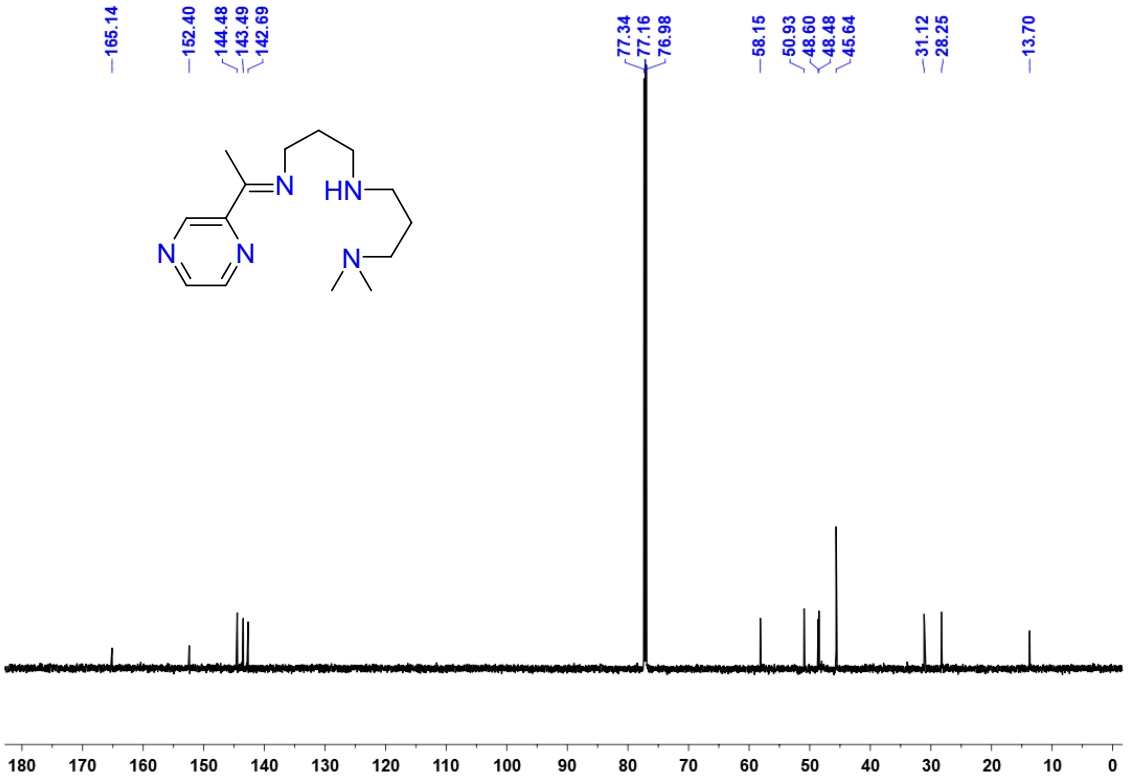

Fig. S4. ^{13}C NMR of (*E*)-N^1,N^1-dimethyl-N^3-(3-((1-(pyrazin-2 yl)ethylidene)amino)propyl)propane-1,3-diamine (**L²**) in $CDCl_3$ at r.t.

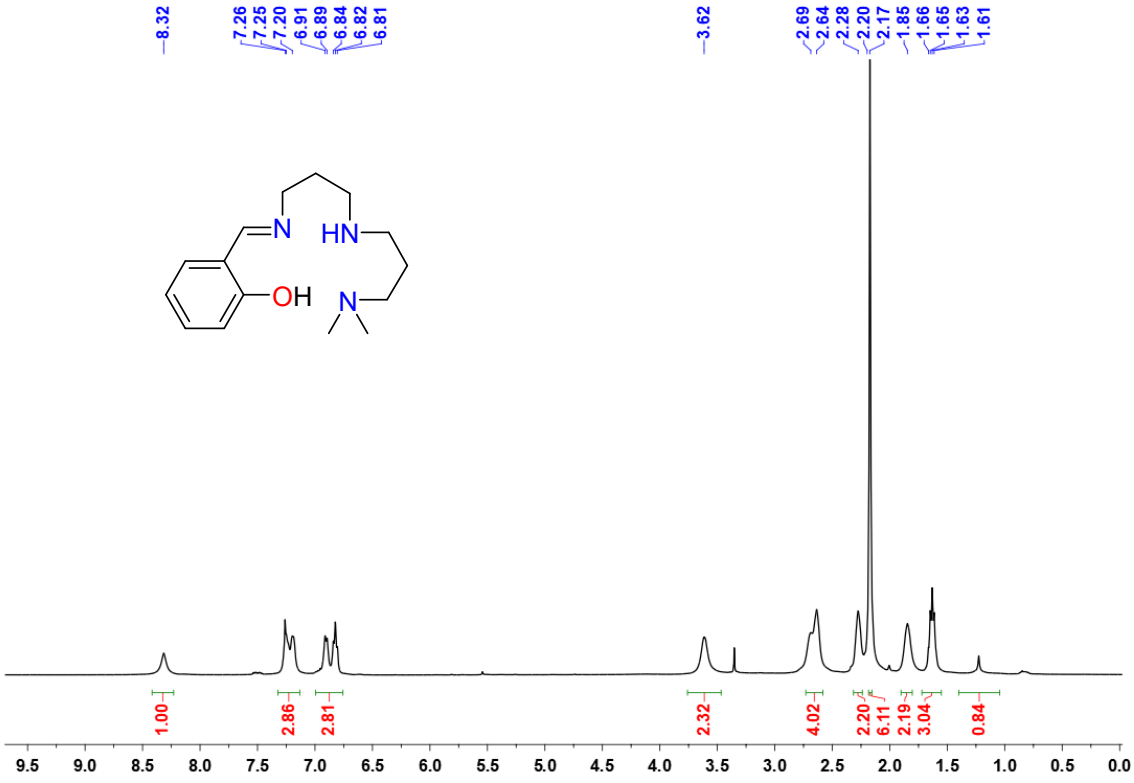

Fig. S5. ^{1}H NMR of (*E*)-2-(((3-((3-(dimethylamino)propyl)amino)propyl)imino)methyl)phenol (**HL^{3}**) in $CDCl_3$ at r.t.

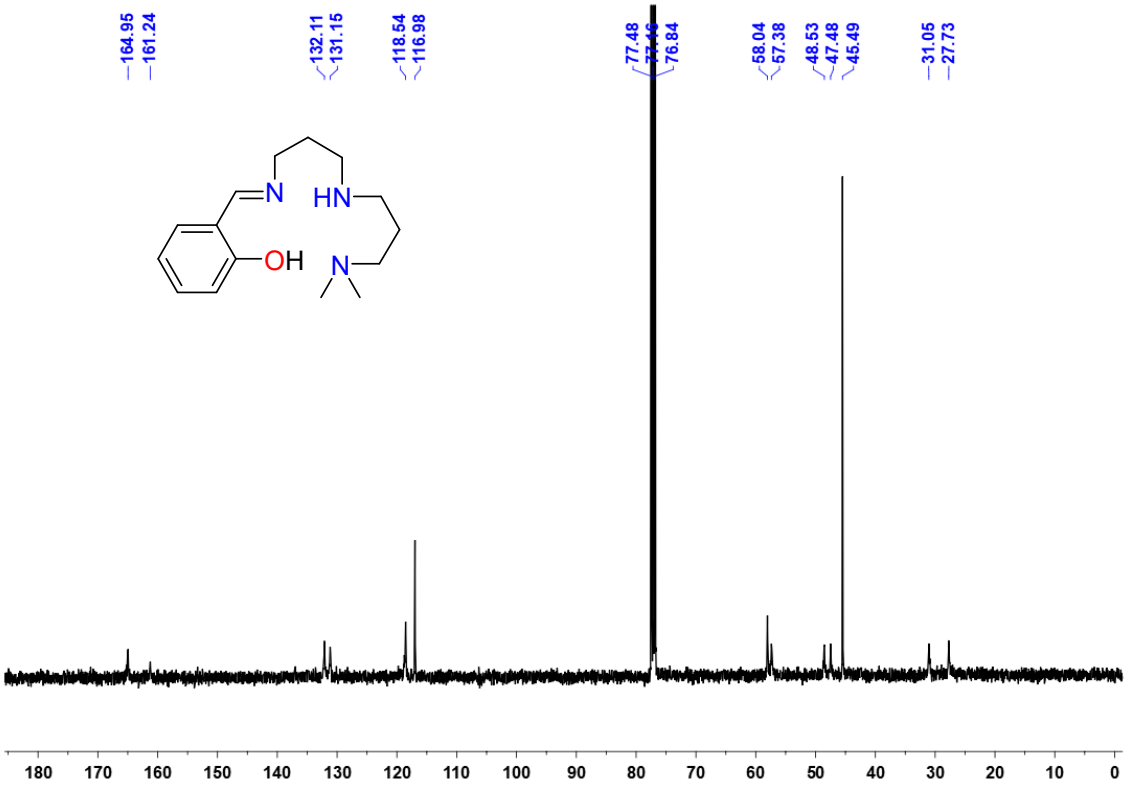

Fig. S6. ^{13}C NMR of (*E*)-2-(((3-((3-(dimethylamino)propyl)amino)propyl)imino)methyl)phenol (**HL^{3}**) in $CDCl_3$ at r.t.

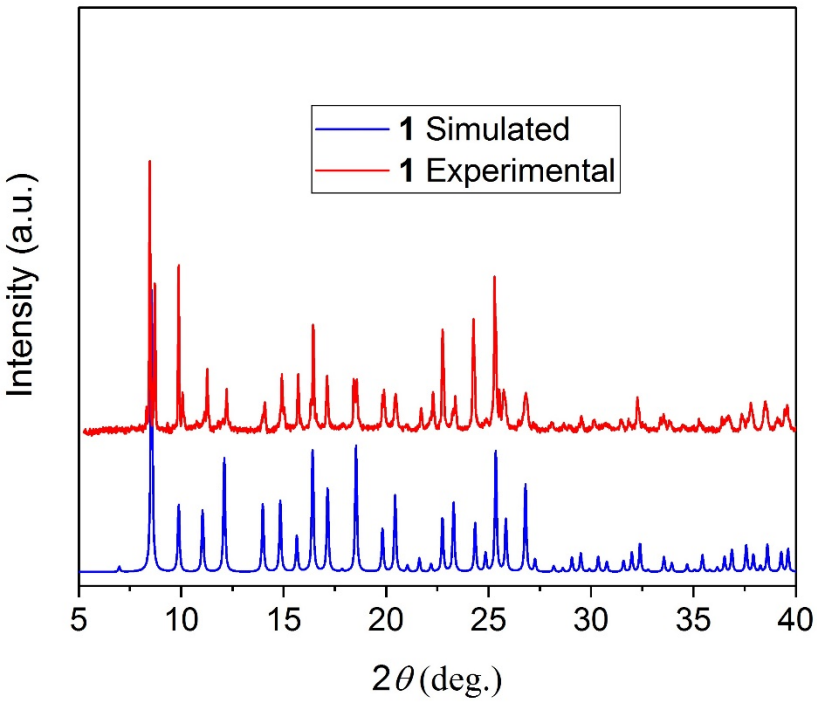

Fig. S7. PXRD of complex **1**

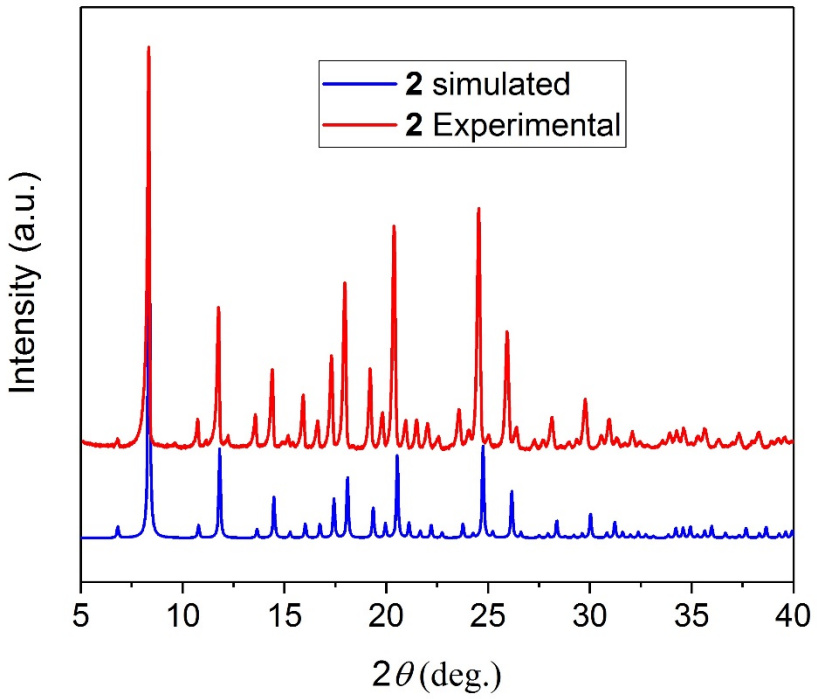

Fig. S8. PXRD of complex **2**

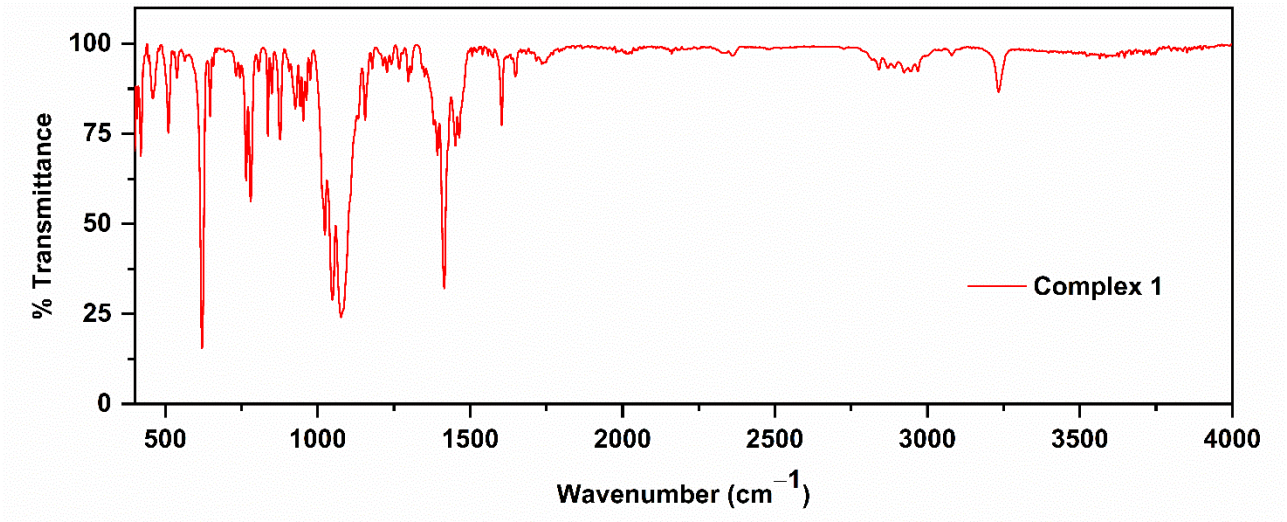

Fig. S9. FT-IR spectrum of complex **1.**

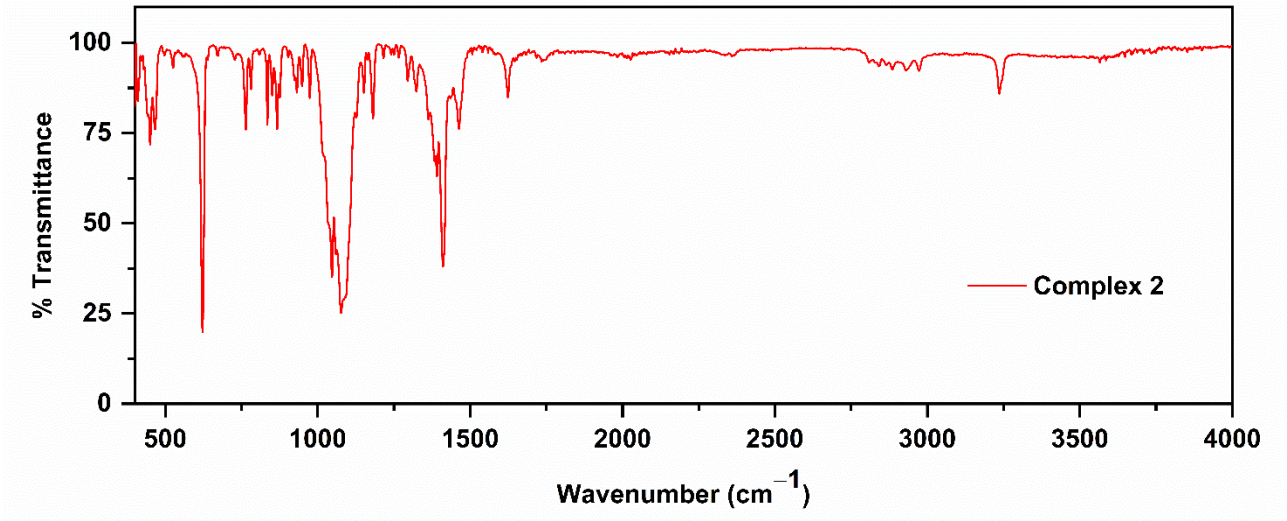

Fig. S10. FT-IR spectrum of complex **2.**

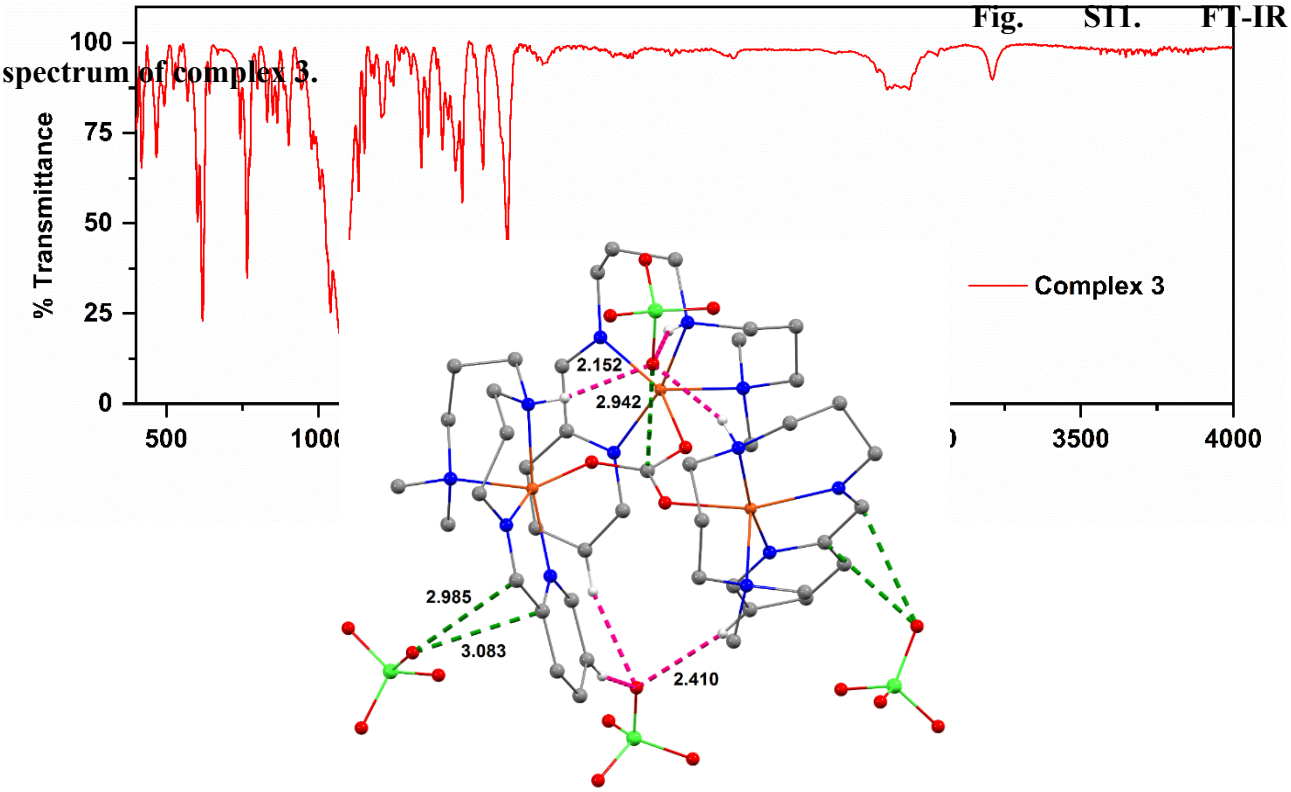

Fig. S11. FT-IR spectrum of complex 3.

Fig.. S12. A part of the packing of complex **1** showing hydrogen bonging and anion−π interactions

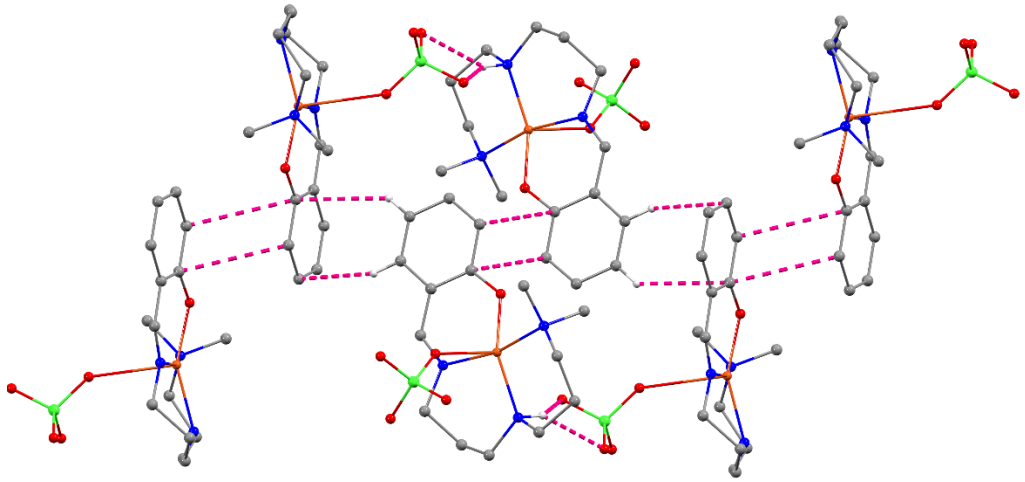

Fig.. S13. A part of crystal packing of **3** showing hydrogen bonding, C−H···π and π−π stacking interactions

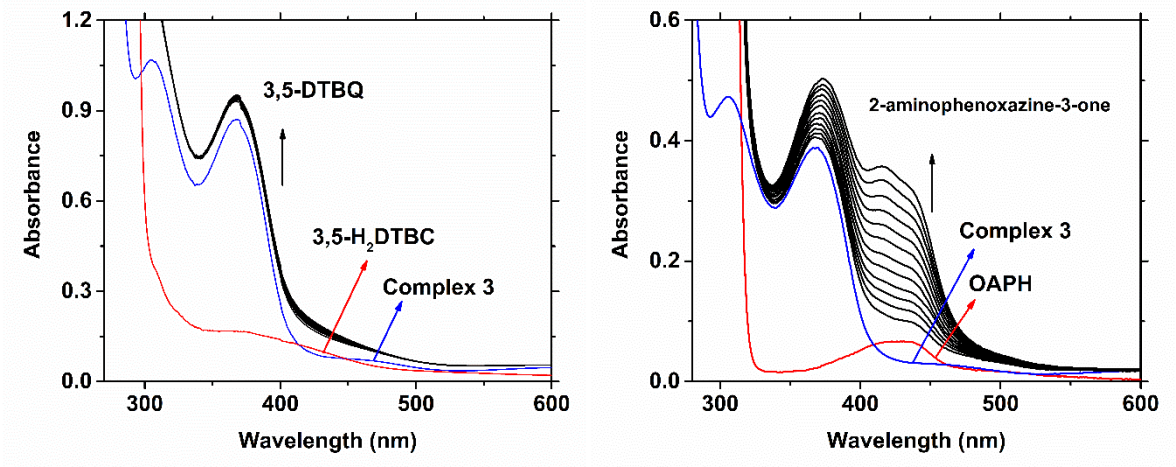

Fig. S14. Time resolved spectral profiles for the oxidation of substrates modelling function of CAO and PHS catalysed by complex **3** in air-saturated methanol.

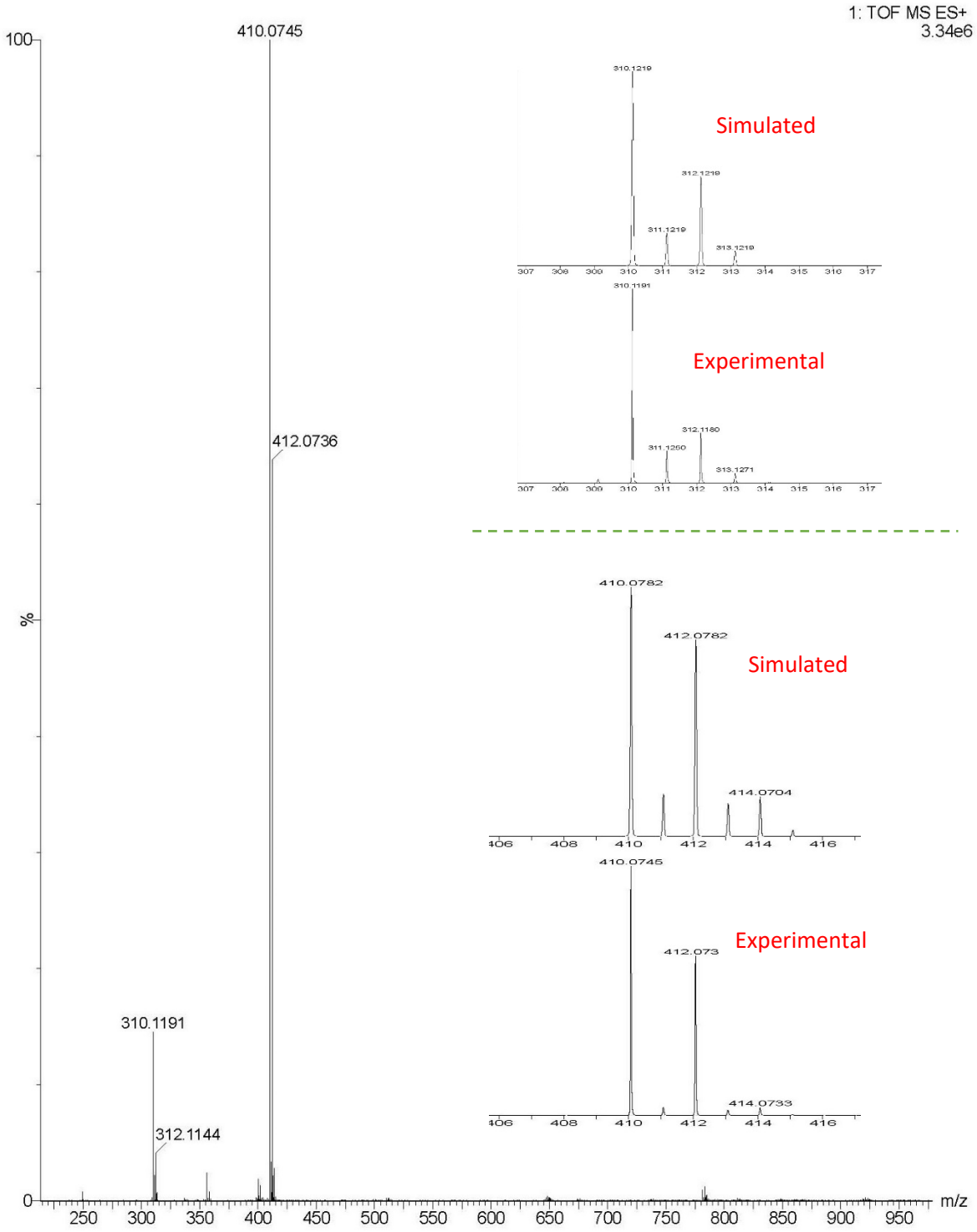

Fig. S15. HR-MS data of complex **1** in methanol showing *m/z* = 410.0745 for species $[Cu^{II}(L^1)(ClO_4)]^+$ (calculated *m/z* = 410.0782) and *m/z* = 310.1191 for species $[Cu^{II}(L^1)–H]^+$ (calculated *m/z* = 310.1210).

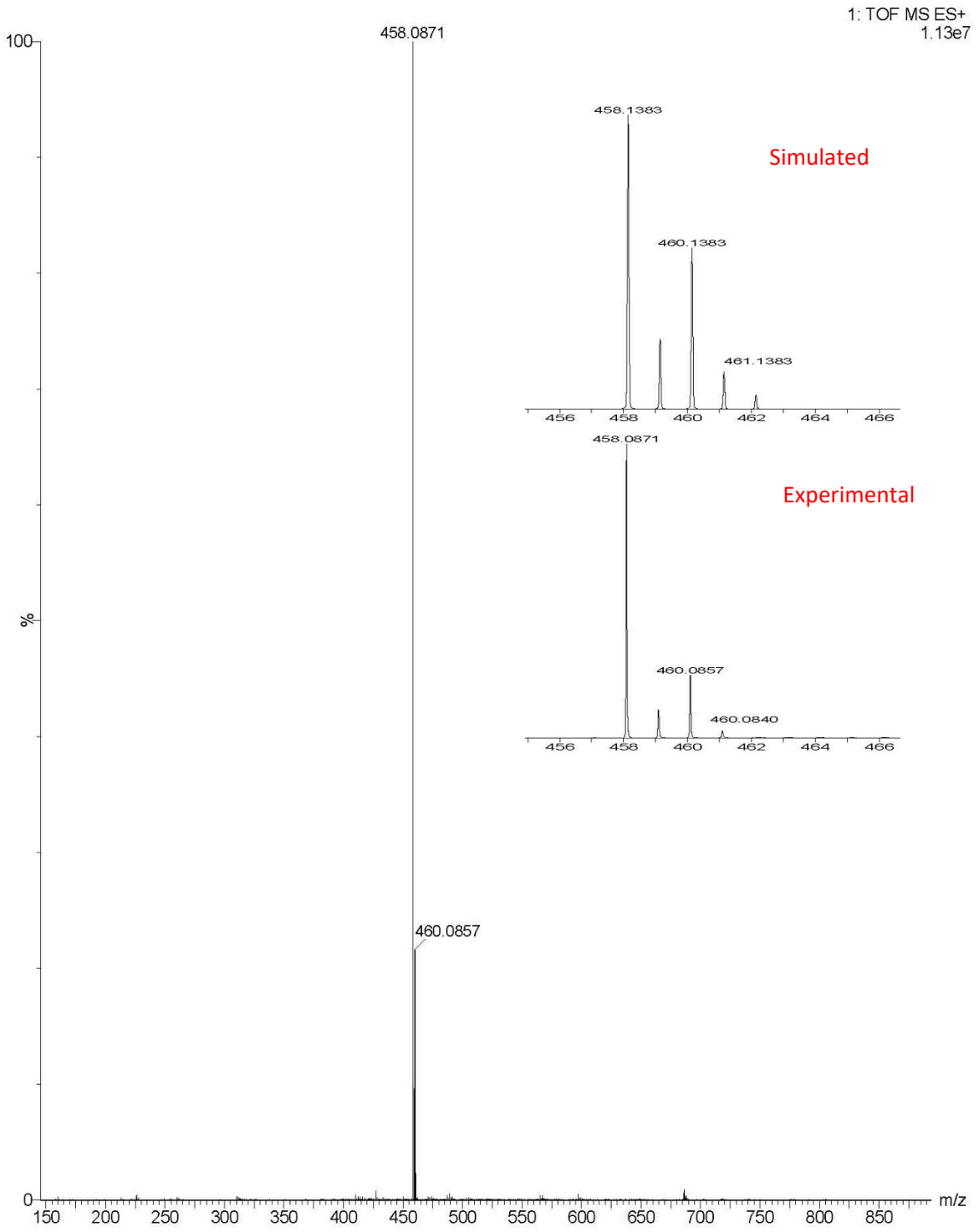

Fig. S16. HR-MS data of complex **1** in presence of *o*-aminophenol in methanol showing *m/z* = 458.0871 for complex-substrate intermediate species $[KCu(L^1)(OAP)]^+$ (calculated *m/z* = 458.1363).

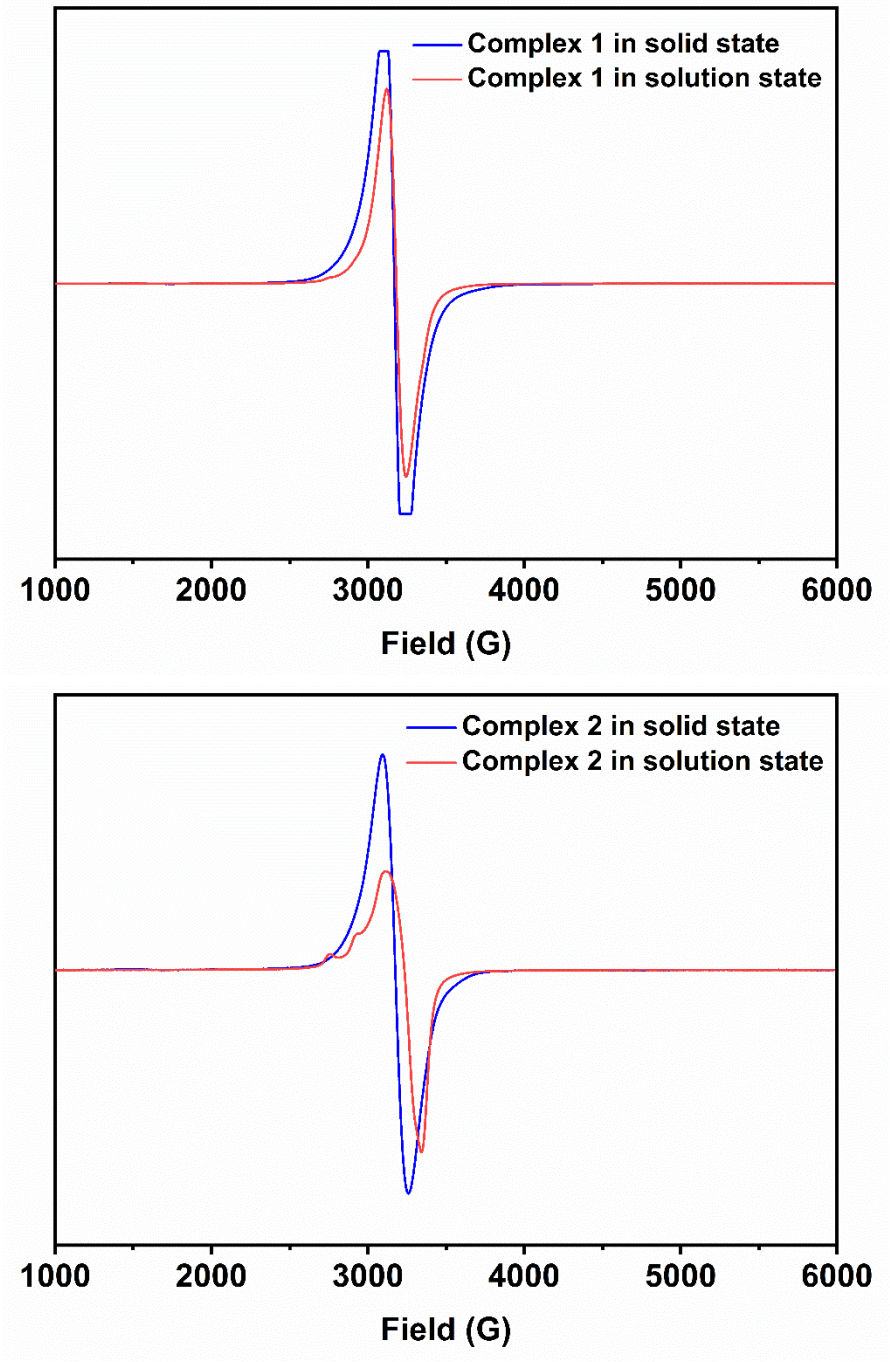

Fig. S17. EPR spectra of complex **1** and **2** in both solid and solution state as well. (frequency = 9.44 GHz; modulation = 1.0 mT; power = 0.841 mW).

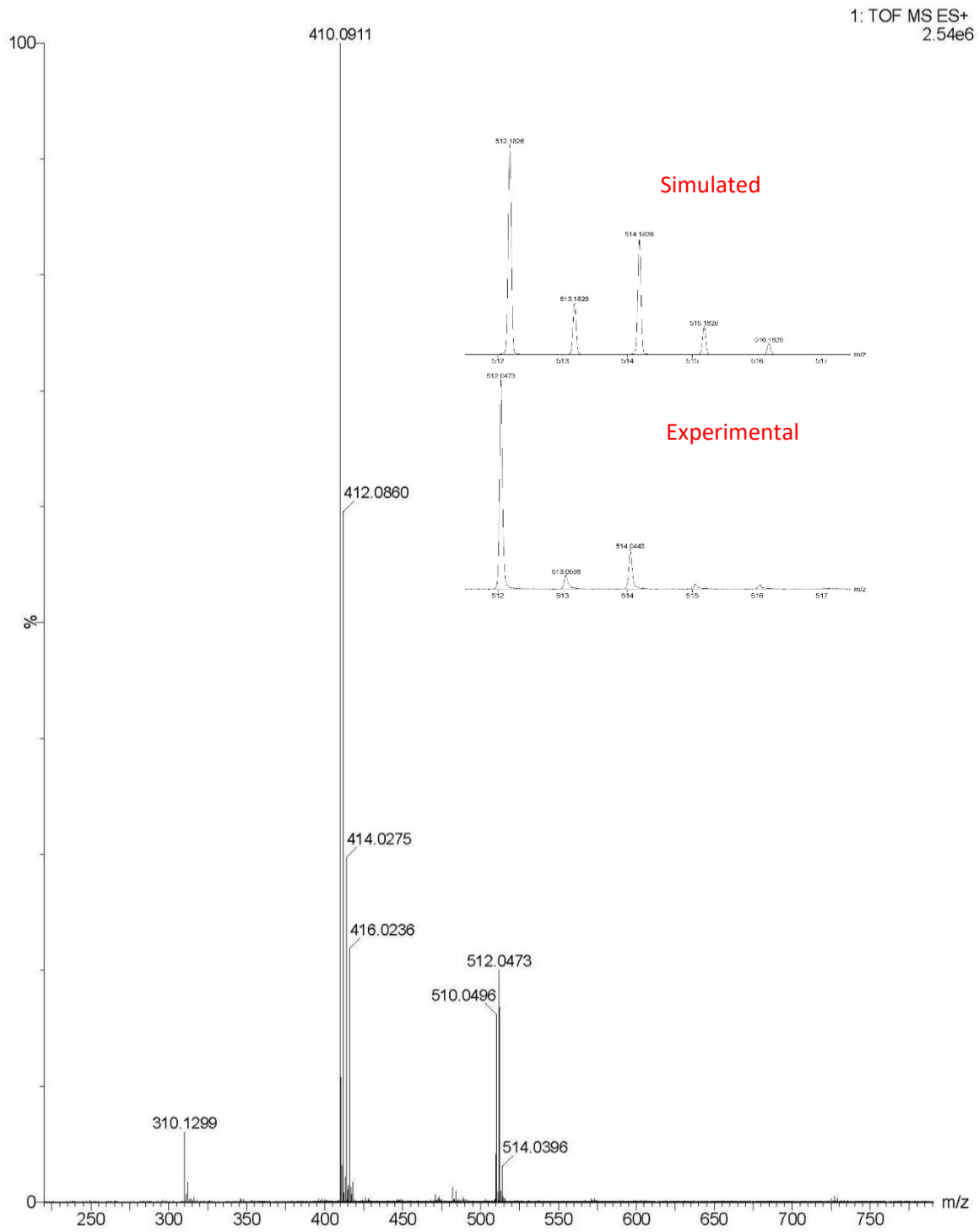

Fig. S18. HR-MS data of complex **1** in presence of benzyl alcohol in methanol.

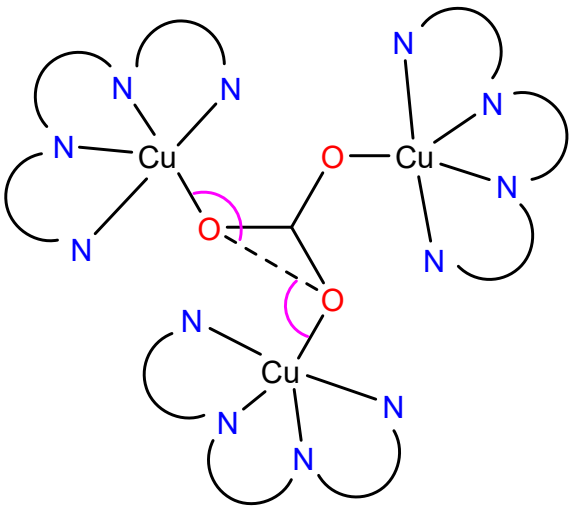

Scheme S1. Bond angles those are important for magneto-structural correlation.

Crystal structure description of dinuclear carbonato-bridged complex (2-I)

Complex **2-I** crystallized in the monoclinic crystal system having $P2_1/n$ space group and the asymmetric unit consists of a dinuclear $[Cu_2(L^2)_2(\mu_2\text{-}CO_3)]^{2+}$ complex cation, two perchlorate counter anions and a lattice methanol molecule. Each metal centre in the complex cation is coordinated by four donor nitrogen atoms of the Schiff base ligand, and one oxygen atom of the carbonato group, which connects the metal centres in *anti-anti* μ_2 bridging mode. Although, both the metal centres construct CuN_4O coordination spheres with square pyramidal geometry, they experience different degree of distraction from the ideal geometry as suggested by τ values of 0.24 and 0.00 for CuA and CuB, respectively. In both cases, the axial sites are occupied by tertiary amine nitrogen atom with bond distances 2.252(4) and 2.247(4) Å, which are significantly larger than the basal bond distances spanning in the range 2.027(4) to 2.040(3) Å. Therefore, it is a basal–basal bridging system through the *anti-anti* μ_2 bridging carbonate with the intra-dimer Cu…Cu separation of 5.309(1) Å and the shortest inter-dimer metal–metal separation of 8.583(1) Å. The coordination spheres may alternatively be described as a distorted octahedron when taking into account the semi-coordinative CuA–O1 and CuB–O1 separations of 2.603(3) and 2.898(3) Å, respectively, but the acute O–Cu–O bite angles (50.45 and 56.30°) seem to exclude the existence of interaction. The lattice methanol molecule is involved in hydrogen bonging interaction with O1 atom of the carbonate group with O100…O1 separation of 2.702(7) Å.

Table S1. Crystal details and structure refinement parameters of complexes **1−3** and **2-I**.

	1	**2**	**3**	**2-I**
Empirical formula	$C_{43}H_{72}Cl_4Cu_3N_{12}O_{19}$	$C_{43}H_{75}Cl_4Cu_3N_{15}O_{19}$	$C_{15}H_{24}CuClN_3O_5$	$C_{30}H_{54}N_{10}O_{12}Cl_2Cu_2$
Temperature (K)	150(2)	273.15	150(2)	150.15
Formula weight (g mol^{-1})	1393.54	1438.60	425.36	944.81
Crystal system	Cubic	Cubic	Monoclinic	Monoclinic
Space group	$P2_13$	$P2_13$	$P2_1/c$	$P2_1/n$
a (Å)	17.8987(7)	18.3268(3)	16.134(2)	12.1603(10)
b (Å)	17.8987(7)	18.3268(3)	8.0576(12)	14.4352(12)
c (Å)	17.8987(7)	18.3268(3)	14.526(2)	23.543(2)
α (deg)	90	90	90.00	90.00
β (deg)	90	90	108.949(5)	103.676(3)
γ (deg)	90	90	90.00	90.00
volume (Å^3)	5734.1(7)	6155.5(3)	1786.0(4)	4015.5(6)
Z	4	4	4	4
D_{calc} (g cm^{-3})	1.614	1.552	1.582	1.563
μ (mm^{-1})	1.370	1.280	1.404	1.263
F(000)	2884	2980	884	1968.0
θ Range (deg)	2.276−27.171	3.335−31.835	2.829−25.242	1.688−26.393
Reflections collected	158178	26464	64147	46611
Independent reflections (R_{int})	4250(0.0669)	5816 (0.0634)	5545(0.0281)	8224 (0.0583)
Observed reflections [I>2σ(I)]	4050	5816	5545	8224
Restraints/parameters	0/250	0/272	0/242	2/521
Goodness-of-fit on $F2$	1.056	1.051	1.061	1.067
Final R indices [I>2σ(I)]	R_1 = 0.0294, wR_2 =0.0737	R_1 = 0.0403, wR_2 =0.0881	R_1 = 0.0431, wR_2 =0.1092	R_1 = 0.0537, wR_2 =0.1236
R indices (all data)	R_1 = 0.0325, wR_2 =0.0755	R_1 = 0.0632, wR_2 =0.0967	R_1 = 0.0502, wR_2 =0.1137	R_1 = 0.0908, wR_2 =0.1389
Largest diff. peak/hole (e Å^{-3})	1.462/−0.492	0.38/−0.28	1.552/−0.867	1.16/−0.71

Table S2. Selected bond angles for complexes **1–3.**

	1	**2**	**2-I**			
			CuA		CuB	
O1 Cu N1	92.33(11)	93.19(16)	O2 CuA N1A	88.92(13)	O3 CuB N4B	93.05(9)
O1 Cu N2	154.43(11)	155.35(16)	O2 CuA N4A	90.02(14)	O3 CuB N3B	162.76(14)
O1 Cu N3	89.34(12)	87.35(16)	N1A CuA N4A	168.45(15)	N4B CuB N3B	96.02(11)
O1 Cu N4	98.86(11)	98.73(17)	O2 CuA N3A	154.05(13)	O3 CuB N1B	87.99(14)
N1 Cu N2	79.52(13)	80.06(18)	N1A CuA N3A	79.60(14)	N4B CuB N1B	162.89(11)
N1 Cu N3	166.39(13)	169.45(18)	N4A CuA N3A	96.62(15)	N3B CuB N1B	79.08(15)
N1 Cu N4	99.59(12)	96.57(18)	O2 CuA N5A	100.02(12)	O3 CuB N5B	93.82(14)
N2 Cu N3	93.26(13)	95.11(18)	N1A CuA N5A	98.07(14)	N4B CuB N5B	96.08(12)
N2 Cu N4	106.35(12)	105.56(18)	N4A CuA N5A	93.44(15)	N3B CuB N5B	99.74(15)
N3 Cu N4	93.49(12)	93.75(18)	N3A CuA N5A	104.56(13)	N1B CuB N5B	100.90(16)
C1 O1 Cu	120.79(15)	125.6(2)	C1 O2 CuA	105.1(3)	C1 O3 CuB	115.9(3)
3						
O1 Cu N1	90.62(7)					
O1 Cu N2	153.36(9)					
N1 Cu N2	97.13(9)					
O1 Cu N3	82.68(7)					
N1 Cu N3	165.82(8)					
N2 Cu N3	94.39(9)					

Table S3. Magneto-structural data for syn-anti carbonato bridged trinuclear copper(II) complexes[a]

Compound	J (cm^{-1})[b]	Cu–O (Å)[c]	(Cu_1OO) (°)	(Cu_2OO) (°)	Ref.
$[Cu_3(L^4)_3(\mu_3\text{-}CO_3)(ClO_4)_3](ClO_4)$	48	1.97	78.6	231.3	S1
$[Cu_3(dmbpy)_3(\mu_3\text{-}CO_3)](BF_4)_4$	29.3	1.98	77–96.3	204.5–220.9	S2
$[Cu_3(MePEA)_3(\mu_3\text{-}CO_3)(ClO_4)_3](ClO_4)$	18.0	1.97	81.0	219.0	S3
$[Cu3(L^5)3(\mu_3\text{-}CO_3)](ClO_4)_4$	17.2	2.00	82.1	217.9	S4
$[Cu3(Medpt)_3(\mu_3\text{-}CO_3)(ClO_4)_3](ClO_4)$	12.6	1.97	88.7	211.7	S5
$[Cu_3(dpt)_3(\mu_3\text{-}CO_3)(ClO_4)_2(H_2O)](ClO_4)$	12.6	1.99	87.0–110.4	199.0–213.3	S6
$[Cu_3(L^6)_3(\mu_3\text{-}CO_3)](ClO_4)_4$	11.3	1.98	87.8	212.2	S7
$[Cu_3(bpy)_6(\mu_3\text{-}CO_3)](BF_4)_4$	10.6	2.02	78.5–88.4	212.7–223.5	S8
$[Cu_3(L^7)_3(\mu_3\text{-}CO_3)(H_2O)_3](NO_3)_4$	8.2	1.93	97.2	204.3	S9
$[Cu_3(apy)_6(\mu_3\text{-}CO_3)_2]_{2n}(ClO_4)_{2n}\cdot 0.5nCH_3OH$	6.2	1.95	77.6	222.4	S10
$[Cu_3(L^8)(\mu_3\text{-}CO_3)](ClO_4)_4\cdot H_2O$	4.0	1.90	91.3–94.7	205.1–208.6	S11
$[Cu_3(dmMePEA)_3(\mu_3\text{-}CO_3)(ClO_4)_3](ClO_4)$	9.9 –8.8	1.97	78.2	221.8	S12
$[Cu_3(bpy)_6(\mu_3\text{-}CO_3)](B_{12}H_{12})_2\cdot 4.5DMF\cdot 2H_2O$	9.8 –8.2	2.06	76.6–81.8	218.5–223.8	S13
$[Cu_3(L^1)_3(\mu_3\text{-}CO_3)](ClO_4)_3$ (**1**)	14.8	1.98	91.0	209.7	This work
$[Cu_3(L^2)_3(\mu_3\text{-}CO_3)](ClO_4)_3$ (**2**)	8.6	1.98	96.5	206.1	This work

[a] Ligand abbreviation: L^4 = (2-pyridylethyl){2-(1-methylimidazolyl)methyl}methylamine, dmbpy = 4,4′-dimethyl-2,2′-bipyridine, MePEA = methyl(2-(2-pyridyl)ethyl)-(2-pyridylmethyl)amine, L^5 = 1,4,7,10-tetra-azabicyclo(5.5.3)-pentadecane, Medpt = bis(3-aminopropyl)methylamine, dpt = bis(3-aminopropyl)amine, L^6 = N-(2-thiophenoethyl)-N,N-bis(3-aminopropyl)amine, bpy = 2,2′-bipyridine, L^7 = 1,4-dioxa-7,10,13-triazacyclopentadecane, apy = 4-aminopyridine, L^8 = a 2,4,6-triethylbenzene-capped hexaamine macrobicycle with pyridyl spacers, dmMePEA = N-methyl(2-(2-pyridyl)ethyl)-(4-methoxy-3,5-dimethyl-2-pyridylmethyl)amine; b = tabulated following $H = -2JS_1\cdot S_2$ type convention; c = Average distance.

Table S4. The reaction Gibbs energies for OAPH oxidation calculated with PBE0/def2 TZVP/D4/CPCM(methanol) for species based on compounds **1-2**

Reactions for **1** [a]	D_rG (kcal/mol)
$[Cu^{II}(L^1)(H_2O)]^{2+} + OAPH = [Cu^{II}(HL^1)(OAP)]^{2+} + H_2O$	0.557
$[Cu^{II}(HL^1)(OAP)]^{2+} + OH^- = [Cu^{I}(HL^1)(BQMI^{\bullet-})]^{1+} + H_2O$	-22.668
$[Cu^{I}(HL^1)(BQMI^{\bullet-})]^{1+} + O_2 = [Cu^{II}(HL^1)(BQMI^{\bullet-})(O_2^{\bullet-})]^{1+}$	2.156
$[Cu^{II}(HL^1)(BQMI^{\bullet-})(O_2^{\bullet-})]^{1+} = [Cu^{II}(L^1)(OOH)]^{1+} + BQMI$	-6.581
$[Cu^{II}(L^1)(OOH)]^{1+} + H_3O^+ = [Cu^{II}(L^1)(H_2O)]^{2+} + H_2O_2$	-29.230
Reactions for **2** [a]	
$[Cu^{II}(L^2)(H_2O)]^{2+} + OAPH = [Cu^{II}(HL^2)(OAP)]^{2+} + H_2O$	0.231
$[Cu^{II}(HL^2)(OAP)]^{2+} + OH^- = [Cu^{I}(HL^2)(BQMI^{\bullet-})]^{1+} + H_2O$	-25.698
$[Cu^{I}(HL^2)(BQMI^{\bullet-})]^{1+} + O_2 = [Cu^{II}(HL^2)(BQMI^{\bullet-})(O_2^{\bullet-})]^{1+}$	4.174
$[Cu^{II}(HL^2)(BQMI^{\bullet-})(O_2^{\bullet-})]^{1+} = [Cu^{II}(L^2)(OOH)]^{1+} + BQMI$	-6.355
$[Cu^{II}(L^2)(OOH)]^{1+} + H_3O^+ = [Cu^{II}(L^2)(H_2O)]^{2+} + H_2O_2$	-28.118

[a] OAPH = *o*-aminophenol, OAP^- = *o*-aminophenolate anion, BQMI = *o*-iminobenzoquinone, $BQMI^{\bullet-}$ = *o*-iminobenzoquinonate radical anion.

Selected molecular structures of intermediate complexes of **1** overlaid with the spin density distribution:

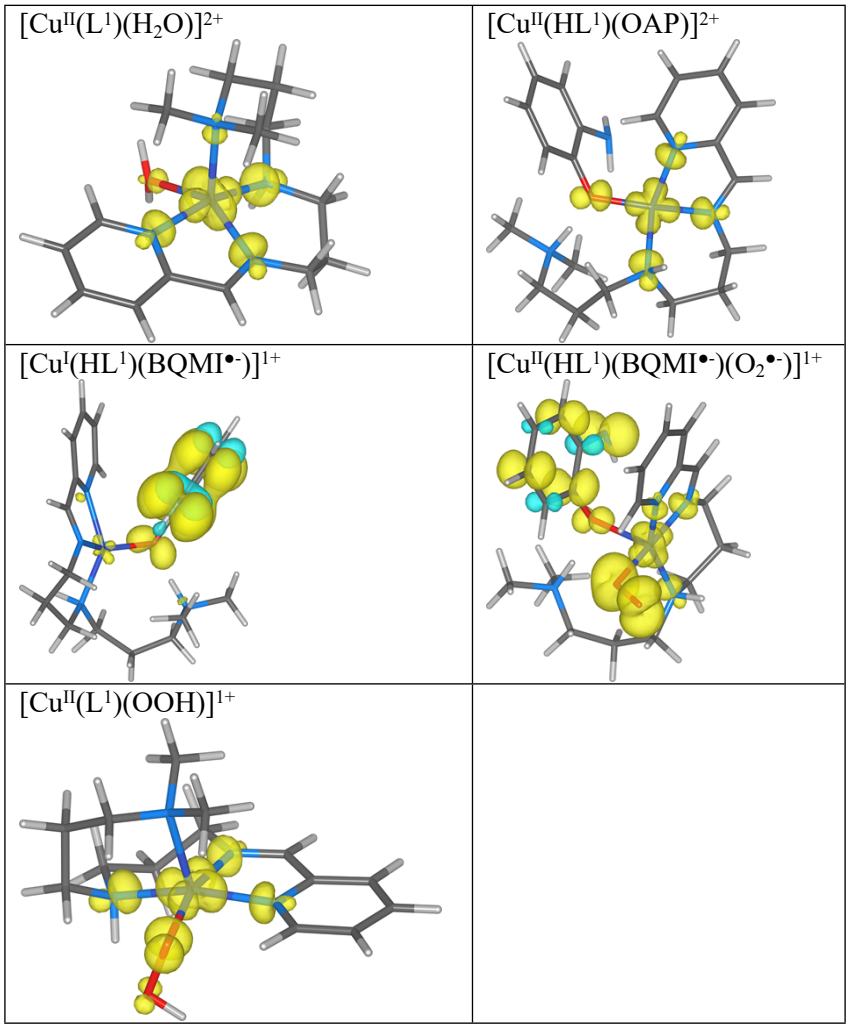

Table S5. The reaction Gibbs energies for benzyl alcohol oxidation calculated with PBE0/def2-TZVP/D4/CPCM (acetonitrile) for species based on compounds **1-2**

Reactions for **1** [a]	D_rG (kcal/mol)
$[Cu^{II}(L^1)(H_2O)]^{2+} + PhCH_2OH = [Cu^{II}(HL^1)(PhCH_2O)]^{2+} + H_2O$	-0.002
$[Cu^{II}(HL^1)(PhCH_2O)]^{2+} + TEMPO = [Cu^{II}(HL^1)(PhCHO^{\bullet-})]^{2+} + TEMPO\text{-}H$	17.195
$[Cu^{II}(HL^1)(PhCHO^{\bullet-})]^{2+} = [Cu^{I}(HL^1)(PhCHO)]^{2+}$	-19.672
$[Cu^{I}(HL^1)(PhCHO)]^{2+} + O_2 = [Cu^{II}(L^1)(OOH)]^{2+} + PhCHO$	8.128
$[Cu^{II}(L^1)(OOH)]^{2+} + TEMPO\text{-}H + H_2O = [Cu^{II}(L^1)(H_2O)]^{2+} + TEMPO + H_2O_2$	-23.242
Reactions for **2** [a]	
$[Cu^{II}(L^2)(H_2O)]^{2+} + PhCH_2OH = [Cu^{II}(HL^2)(PhCH_2O)]^{2+} + H_2O$	-0.033
$[Cu^{II}(HL^2)(PhCH_2O)]^{2+} + TEMPO = [Cu^{II}(HL^2)(PhCHO^{\bullet-})]^{2+} + TEMPO\text{-}H$	17.506
$[Cu^{II}(HL^2)(PhCHO^{\bullet-})]^{2+} = [Cu^{I}(HL^2)(PhCHO)]^{2+}$	-22.491
$[Cu^{I}(HL^2)(PhCHO)]^{2+} + O_2 = [Cu^{II}(L^2)(OOH^{\bullet})]^{2+} + PhCHO$	10.985
$[Cu^{II}(L^2)(OOH^{\bullet})]^{2+} + TEMPO\text{-}H + H_2O = [Cu^{II}(L^2)(H_2O)]^{2+} + TEMPO + H_2O_2$	-23.561

[a] $PhCH_2OH$ = benzyl alcohol, TEMPO = 2,2,6,6-tetramethylpiperidine1-oxyl, TEMPO-H = 1-hydroxy-2,2,6,6-tetramethylpiperidine.

Selected molecular structures of intermediate complexes of **1** overlaid with the spin density distribution:

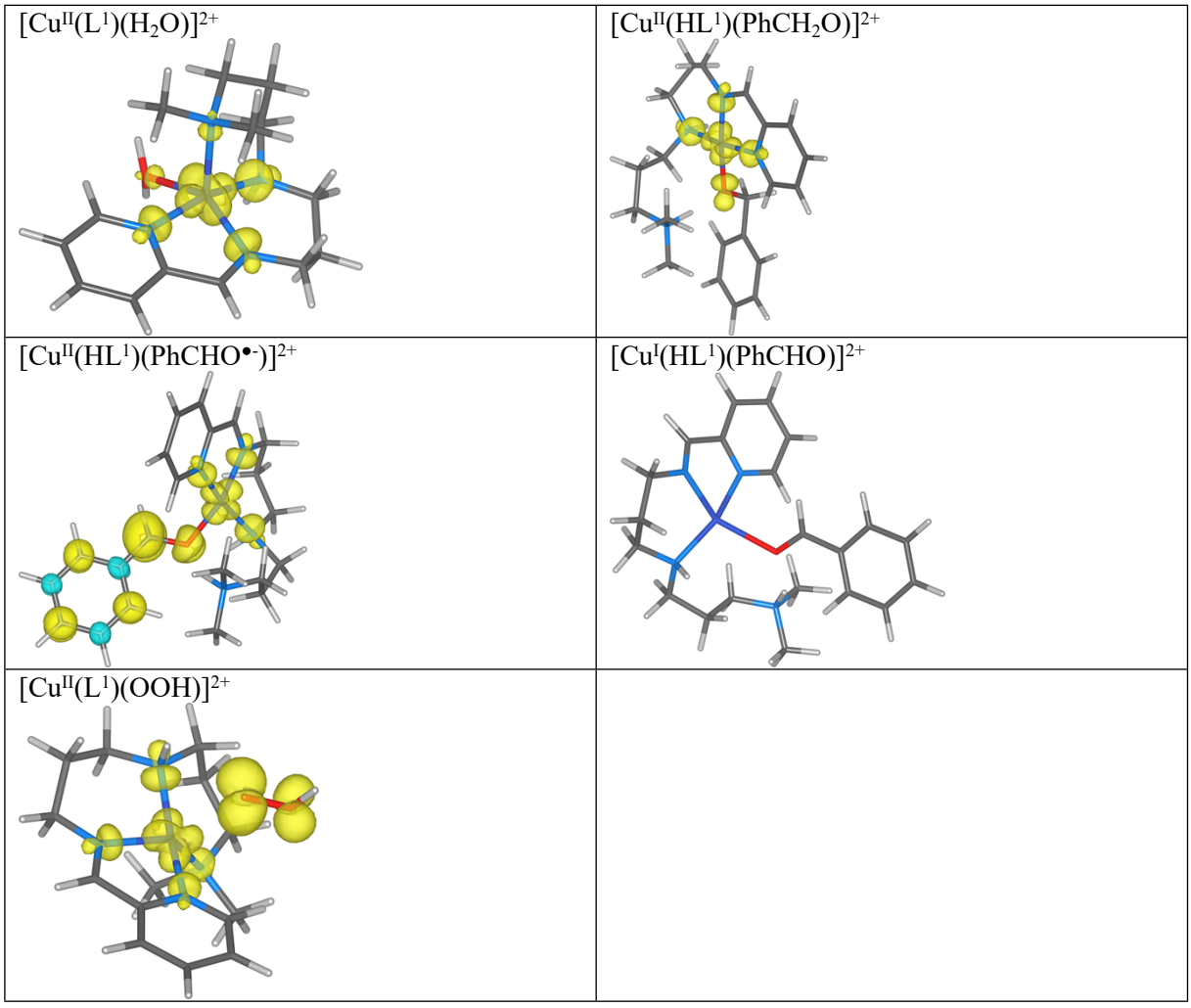

Selected molecular structures of intermediate complexes of **2** overlaid with the spin density distribution:

$[Cu^{II}(L^2)(H_2O)]^{2+}$ 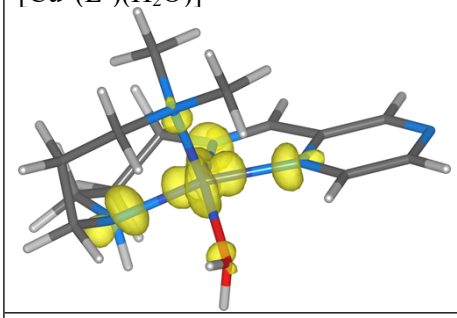	$[Cu^{II}(HL^2)(PhCH_2O)]^{2+}$ 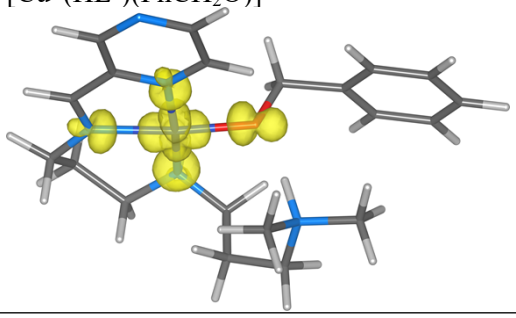
$[Cu^{II}(HL^2)(PhCHO^{\bullet -})]^{2+}$ 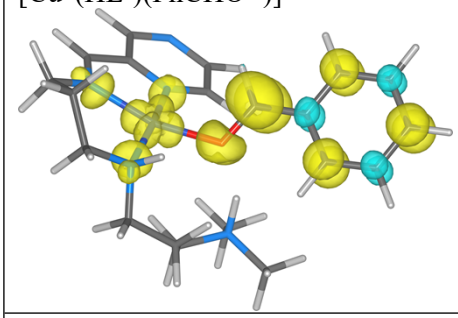	$[Cu^{I}(HL^2)(PhCHO)]^{2+}$ 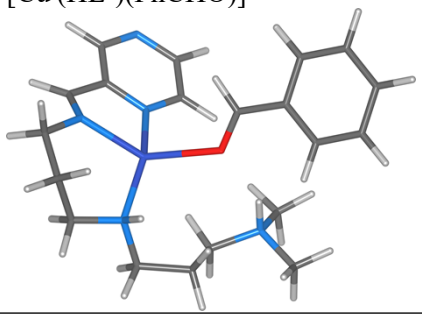
$[Cu^{II}(L^2)(OOH)]^{2+}$ 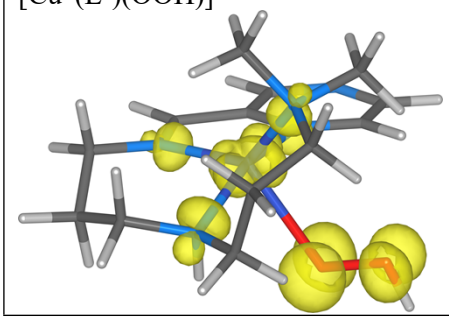	

NMR data of the products:

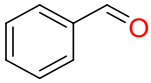

benzaldehyde (**P**): Isolated as colourless liquid (50 mg, 96%). ^{1}H NMR (400 MHz, $CDCl_3$) δ 10.01 (s, 1H), 7.92 – 7.84 (m, 2H), 7.67 – 7.57 (m, 1H), 7.52 (t, *J* = 7.5 Hz, 2H). ^{13}C NMR (101 MHz, $CDCl_3$) δ 192.50, 136.49, 134.56, 129.83, 129.09.

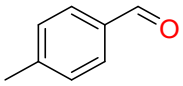

4-methylbenzaldehyde (**P_1**): Isolated as white solid (56 mg, 95%). ^{1}H NMR (400 MHz, $CDCl_3$) δ 9.97 (s, 1H), 7.79 (d, *J* = 8.1 Hz, 2H), 7.34 (d, *J* = 7.9 Hz, 2H), 2.45 (s, 3H). ^{13}C NMR (101 MHz, $CDCl_3$) δ 191.99, 145.52, 134.18, 129.75, 21.85.

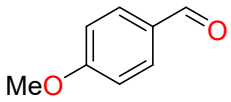

4-methoxybenzaldehyde (**P_2**): Isolated as white solid (65 mg, 96%). ^{1}H NMR (400 MHz, $CDCl_3$) δ 9.90 (s, 1H), 7.86 (d, *J* = 8.6 Hz, 2H), 7.02 (d, *J* = 8.6 Hz, 2H), 3.91 (s, 3H). ^{13}C NMR (101 MHz, $CDCl_3$) δ 190.03, 163.79, 131.18, 129.13, 113.52, 54.85.

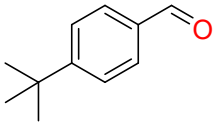

4-(*tert*-butyl)benzaldehyde (**P_3**): Isolated as white solid (80 mg, 99%). ^{1}H NMR (700 MHz, $CDCl_3$) δ 10.09 (s, 1H), 7.93 (d, *J* = 7.3 Hz, 2H), 7.67 (d, *J* = 7.3 Hz, 2H), 1.47 (s, 9H). ^{13}C NMR (176 MHz, $CDCl_3$) δ 189.96, 156.29, 131.95, 127.61, 123.88, 33.17, 28.98.

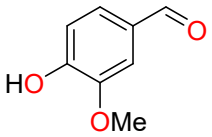

4-hydroxy-3-methoxybenzaldehyde (**P_4**): Isolated as white solid (75 mg, 99%). ^{1}H NMR (400 MHz, $CDCl_3$) δ 9.80 (s, 1H), 7.41 (d, *J* = 5.4 Hz, 2H), 7.02 (d, *J* = 8.3 Hz, 1H), 6.62 (s, 1H), 3.92 (s, 3H). ^{13}C NMR (101 MHz, $CDCl_3$) δ 190.96, 151.73, 147.16, 129.59, 127.41, 114.46, 108.81, 55.96.

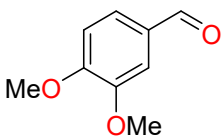

Veratraldehyde (**P_5**): Isolated as white solid (82 mg, 99%). ^{1}H NMR (400 MHz, $CDCl_3$) δ 9.94 (s, 1H), 7.68 – 7.40 (m, 2H), 7.07 (d, *J* = 7.8 Hz, 1H), 4.05 (s, 3H), 4.03 (s, 3H). ^{13}C NMR (101 MHz, $CDCl_3$) δ 188.91, 152.42, 147.55, 128.08, 124.89, 108.46, 106.90, 54.34, 54.08.

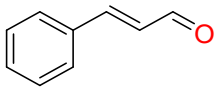

cinnamaldehyde (**P_6**): Isolated as white solid (62 mg, 97%). ^{1}H NMR (700 MHz, $CDCl_3$) δ 9.71 (d, *J* = 7.7 Hz, 1H), 7.57 (dd, *J* = 7.0 Hz, 2H), 7.48 (d, *J* = 15.9 Hz, 1H), 7.44 (t, *J* = 8.7 Hz, 3H), 6.72 (dd, *J* = 15.9 Hz, 1H). ^{13}C NMR (176 MHz, $CDCl_3$) δ 193.87, 152.95, 134.14, 131.41, 129.24, 128.68.

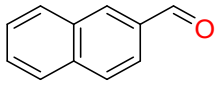

2-naphthaldehyde (**P_7**): Isolated as white solid (61 mg, 79%). ^{1}H NMR (400 MHz, $CDCl_3$) δ 10.16 (s, 1H), 8.33 (s, 1H), 8.02 – 7.88 (m, 4H), 7.67 – 7.56 (m, 2H). ^{13}C NMR (101 MHz, $CDCl_3$) δ 192.29, 136.47, 134.58, 134.13, 132.66, 129.55, 129.13, 128.10, 127.11, 122.78.

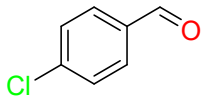

4-chlorobenzaldehyde (**P_8**): Isolated as white solid (54 mg, 77%). ^{1}H NMR (400 MHz, $CDCl_3$) δ 9.98 (s, 1H), 7.92 – 7.76 (m, 2H), 7.51 (d, *J* = 8.4 Hz, 2H). ^{13}C NMR (101 MHz, $CDCl_3$) δ 190.86, 140.94, 134.71, 130.90, 129.46.

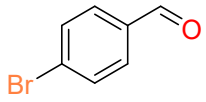

4-bromobenzaldehyde (**P_9**): Isolated as white solid (66 mg, 72%). ^{1}H NMR (700 MHz, $CDCl_3$) δ 9.99 (s, 1H), 7.76 (d, *J* = 8.4 Hz, 2H), 7.70 (d, *J* = 8.3 Hz, 2H). ^{13}C NMR (176 MHz, $CDCl_3$) δ 190.83, 134.82, 132.20, 130.73, 129.52.

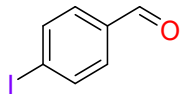

4-iodobenzaldehyde (**P_{10}**): Isolated as white solid (85 mg, 74%). ^{1}H NMR (700 MHz, $CDCl_3$) δ 9.94 (s, 1H), 7.89 (d, *J* = 8.3 Hz, 2H), 7.57 (d, *J* = 8.4 Hz, 2H). ^{13}C NMR (176 MHz, $CDCl_3$) δ 191.49, 138.49, 135.65, 130.89, 102.93.

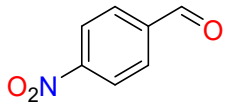

4-nitrobenzaldehyde (**P_{11}**): Isolated as off-white solid (49 mg, 65% in 24h; 71 mg, 94% in 16h). ^{1}H NMR (400 MHz, $CDCl_3$) δ 10.16 (s, 1H), 8.46 – 8.34 (m, 2H), 8.11 – 8.05 (m, 2H). ^{13}C NMR (101 MHz, $CDCl_3$) δ 190.41, 140.17, 132.76, 130.60, 124.43.

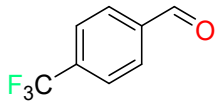

4-(trifluoromethyl)benzaldehyde (**P_{12}**): Isolated as off-white solid (53 mg, 61% in 24h; 79 mg, 91% in 16h). ^{1}H NMR (400 MHz, $CDCl_3$) δ 10.10 (s, 1H), 8.01 (d, *J* = 8.0 Hz, 2H), 7.81 (d, *J* = 8.0 Hz, 2H). ^{13}C NMR (101 MHz, $CDCl_3$) δ 191.26, 130.73, 130.08, 126.28 (q, *J* = 3.7 Hz).

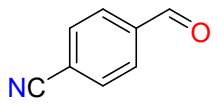

4-formylbenzonitrile (**P_{13}**): Isolated as colourless liquid (36 mg, 55% in 10h; 61 mg, 93% in 24h). ^{1}H NMR (400 MHz, $CDCl_3$) δ 10.09 (s, 1H), 7.99 (d, *J* = 8.0 Hz, 2H), 7.84 (d, *J* = 8.3 Hz, 2H). ^{13}C NMR (101 MHz, $CDCl_3$) δ 190.75, 138.86, 133.02, 130.01, 117.78.

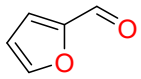

furan-2-carbaldehyde (**P_{14}**): Isolated as colourless liquid solid (30 mg, 62%). ^{1}H NMR (400 MHz, CDCl3) δ 9.68 (s, 1H), 7.70 (s, 1H), 7.26 (d, *J* = 3.4 Hz, 1H), 6.62 (dd, *J* = 3.5 Hz, 1H). ^{13}C NMR (101 MHz, $CDCl_3$) δ 178.06, 153.16, 148.22, 121.12, 112.73.

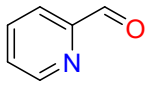

picolinaldehyde (**P_{15}**): Isolated as colourless liquid (17 mg, 32%). ^{1}H NMR (400 MHz, $CDCl_3$) δ 10.08 (s, 1H), 8.79 (d, *J* = 4.7 Hz, 1H), 7.96 (d, *J* = 7.8 Hz, 1H), 7.90 – 7.84 (m, 1H), 7.52 (m, 1H). ^{13}C NMR (101 MHz, $CDCl_3$) δ 193.56, 152.94, 150.34, 137.22, 128.01, 121.85.

NMR spectra of the products:

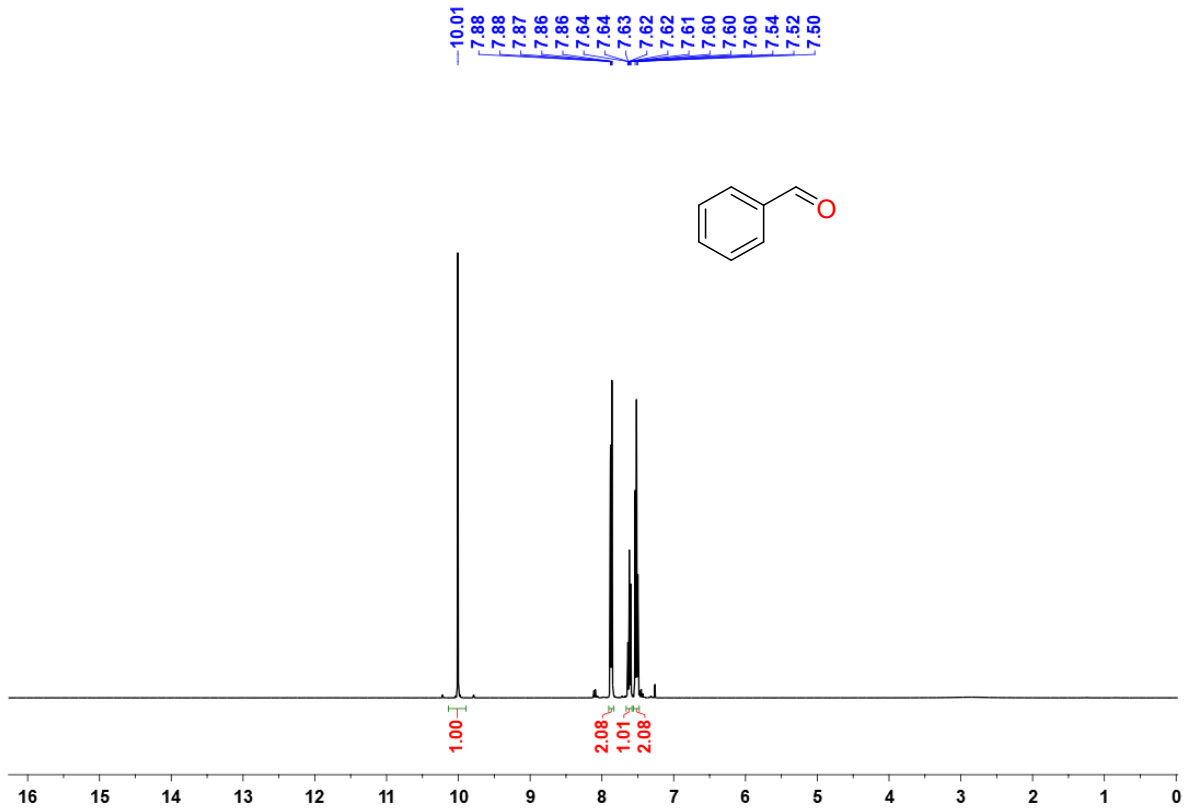

Fig. S19. ^{1}H NMR spectrum of catalytic product benzaldehyde (**P**) in $CDCl_3$ at r.t.

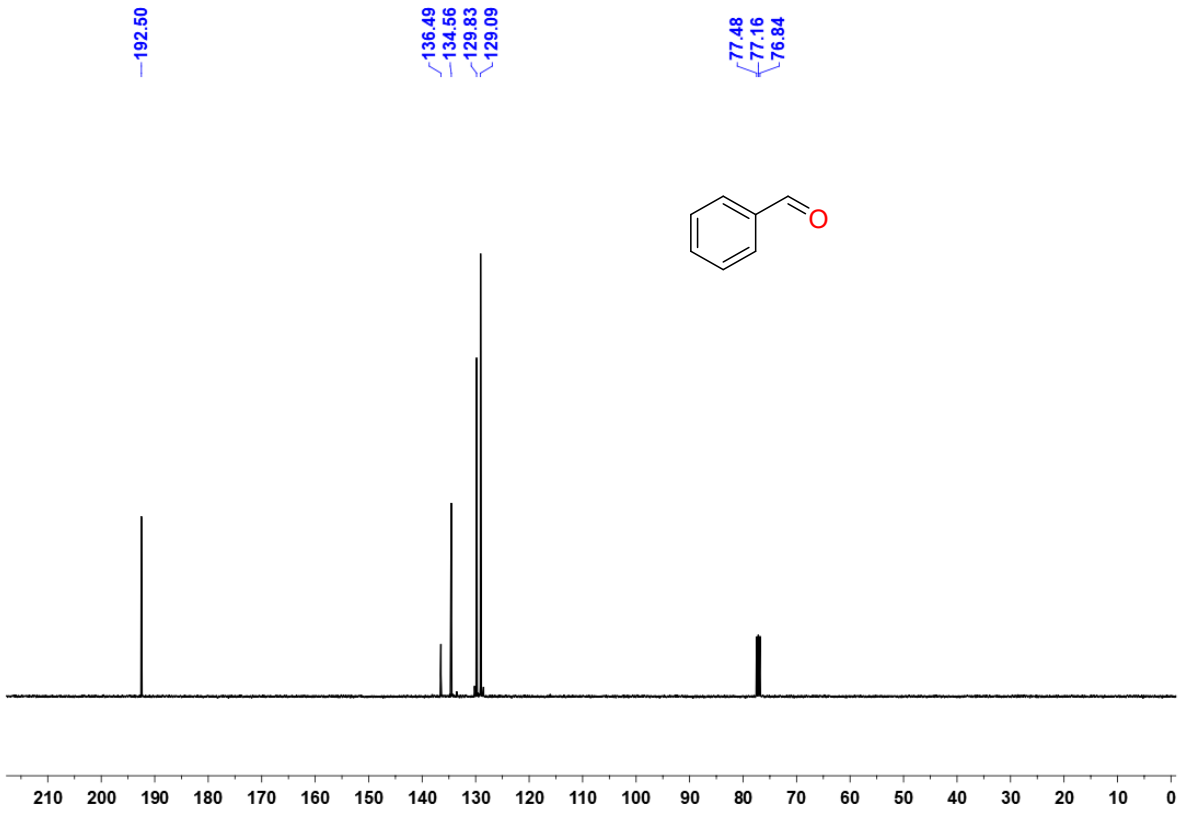

Fig. S20. $^{13}C\{^{1}H\}$ NMR spectrum of catalytic product benzaldehyde (**P**) in $CDCl_3$ at r.t.

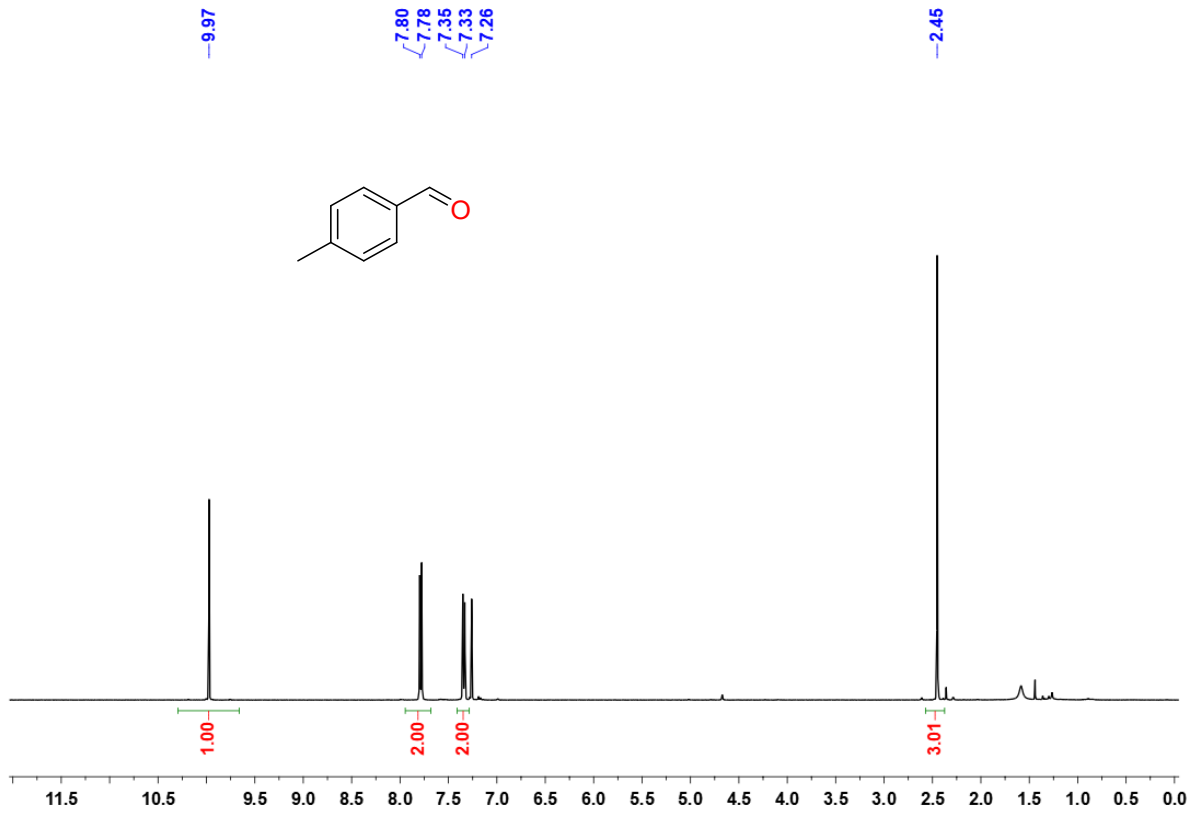

Fig. S21. ^{1}H NMR spectrum of 4-methylbenzaldehyde ($\mathbf{P_1}$) in $CDCl_3$ at r.t.

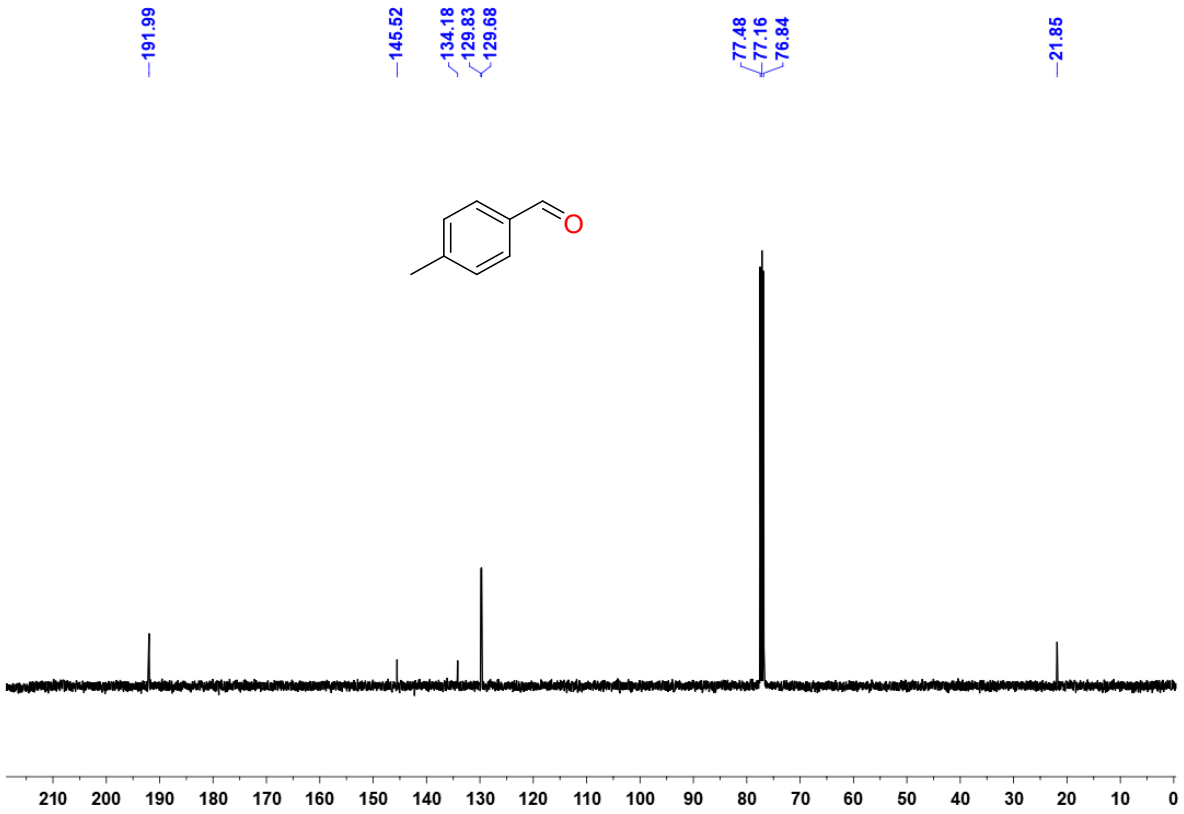

Fig. S22. $^{13}C\{^{1}H\}$ NMR spectrum of 4-methylbenzaldehyde ($\mathbf{P_1}$) in $CDCl_3$ at r.t.

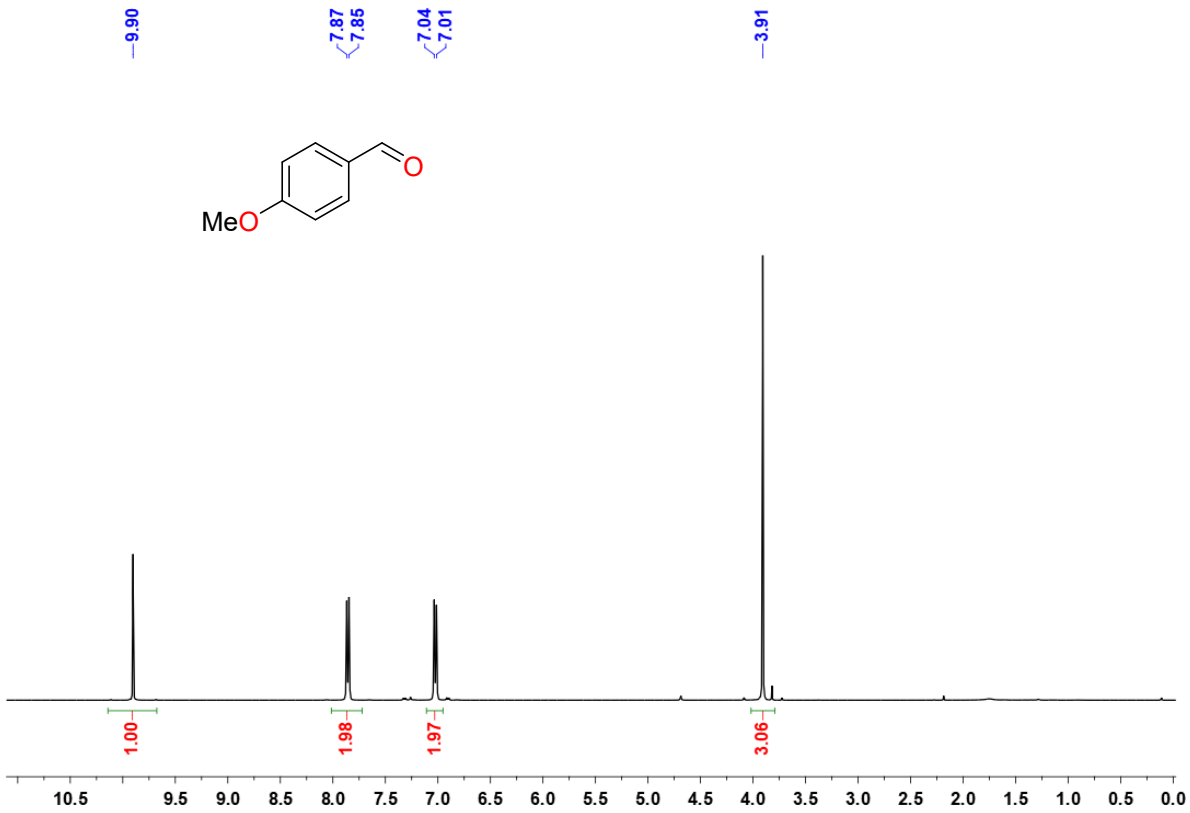

Fig. S23. ^{1}H NMR spectrum of 4-methoxybenzaldehyde (**P$_2$**) in $CDCl_3$ at r.t.

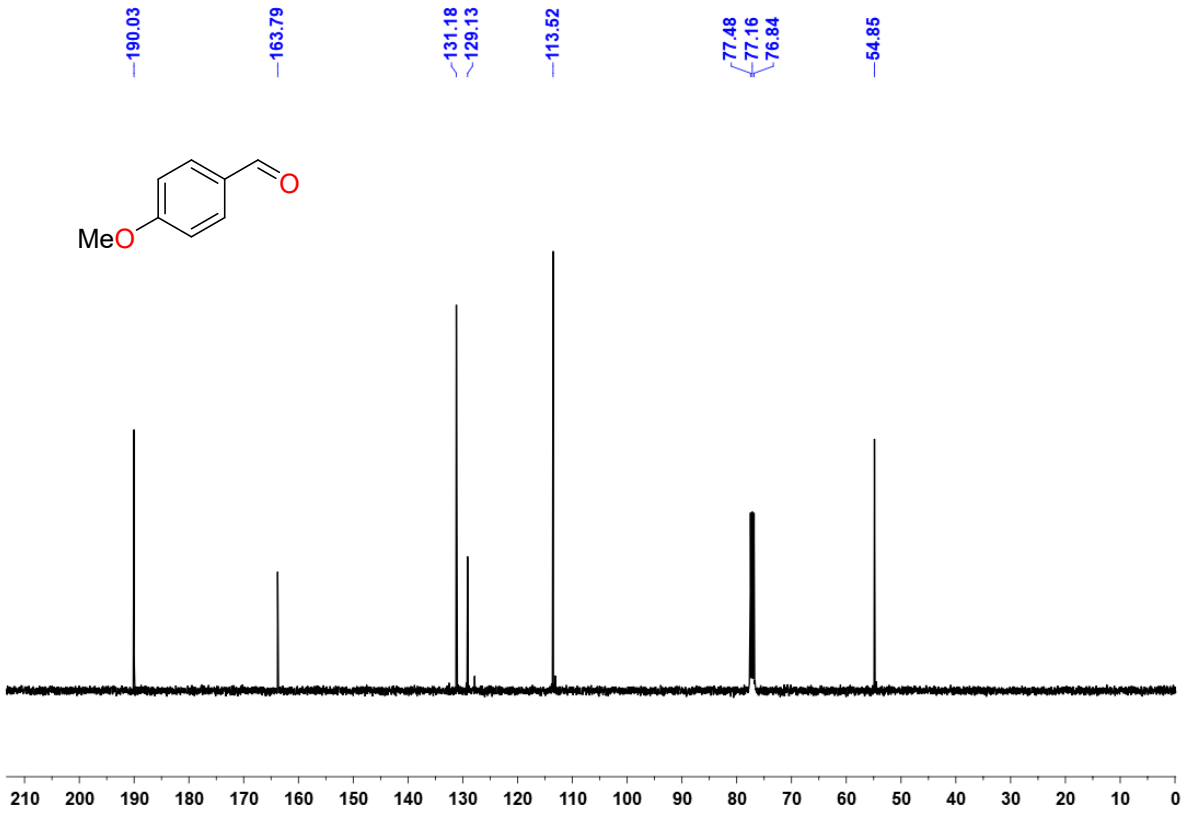

Fig. S24. $^{13}C\{^{1}H\}$ NMR spectrum of 4-methoxybenzaldehyde (**P$_2$**) in $CDCl_3$ at r.t.

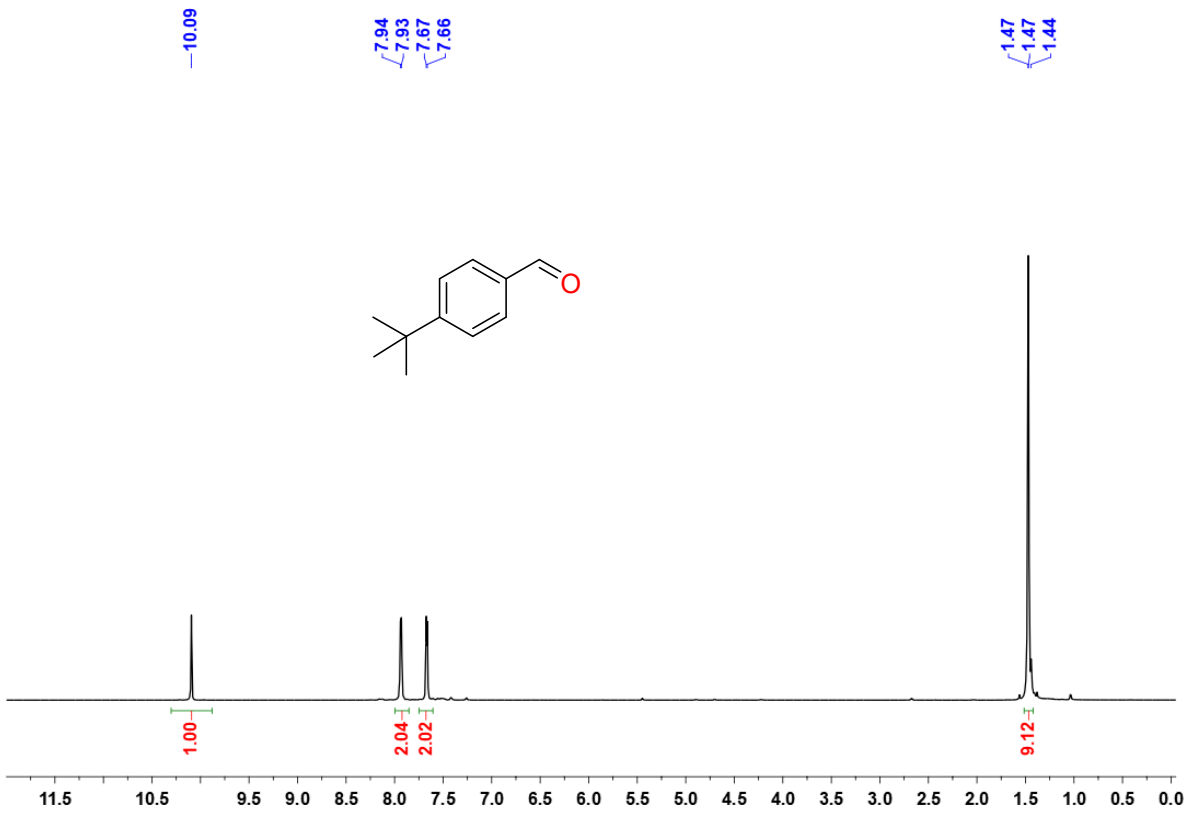

Fig. S25. ^{1}H NMR spectrum of 4-(*tert*-butyl)benzaldehyde (**P$_3$**) in $CDCl_3$ at r.t.

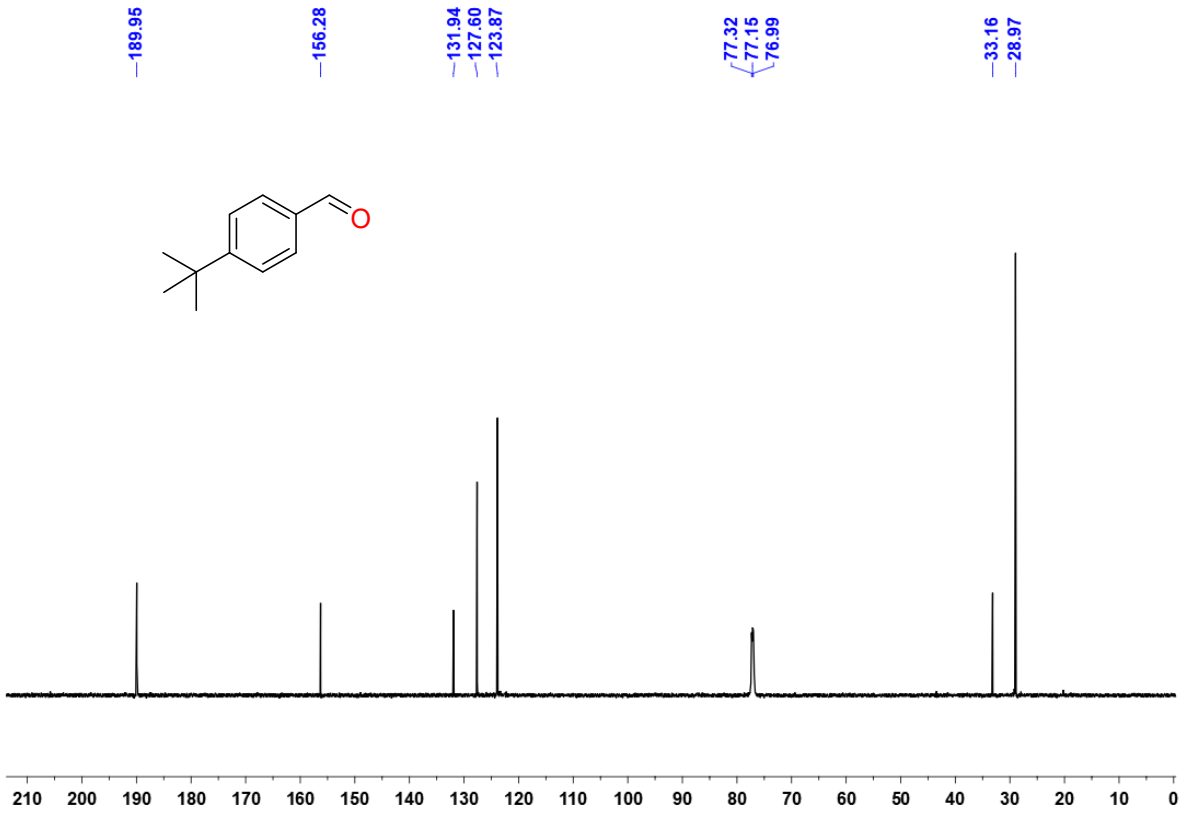

Fig. S26. ^{13}C{^{1}H} NMR spectrum of 4-(*tert*-butyl)benzaldehyde (**P$_3$**) in $CDCl_3$ at r.t.

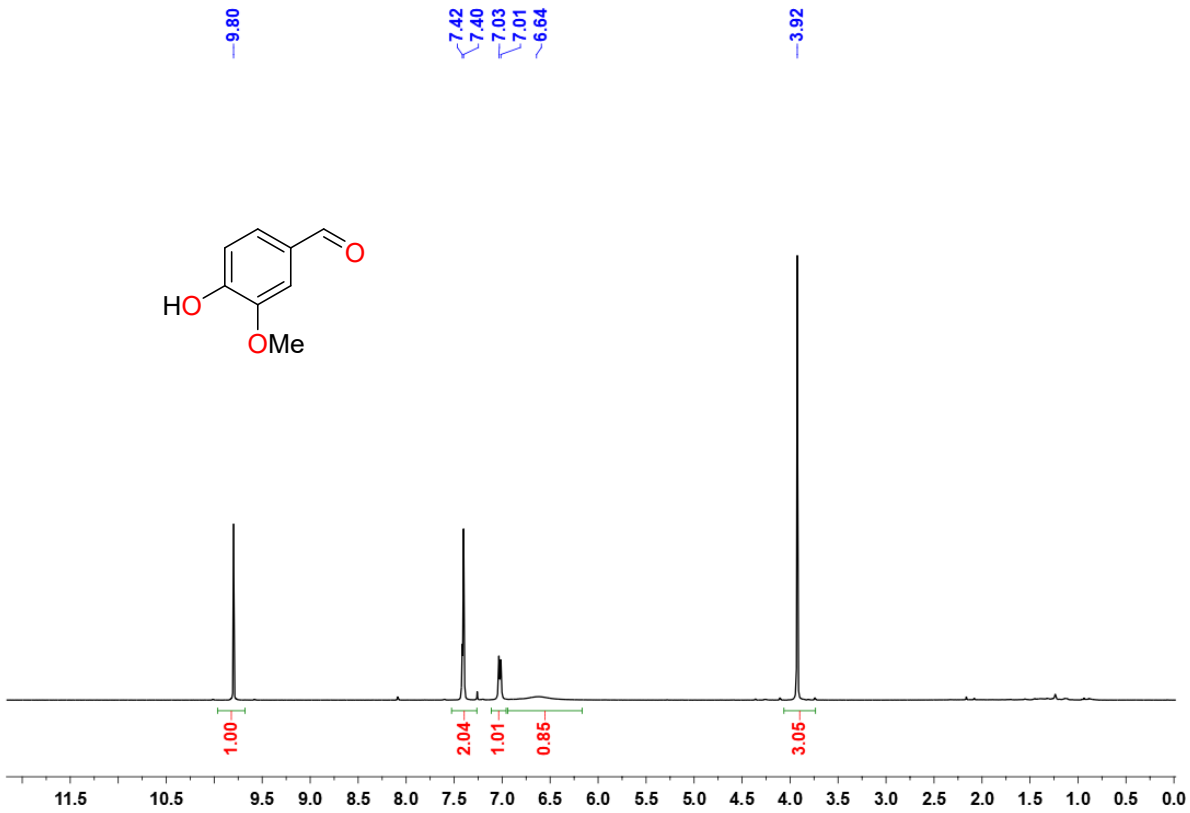

Fig. S27. ^{1}H NMR spectrum of 4-hydroxy-3-methoxybenzaldehyde (**P$_4$**) in $CDCl_3$ at r.t.

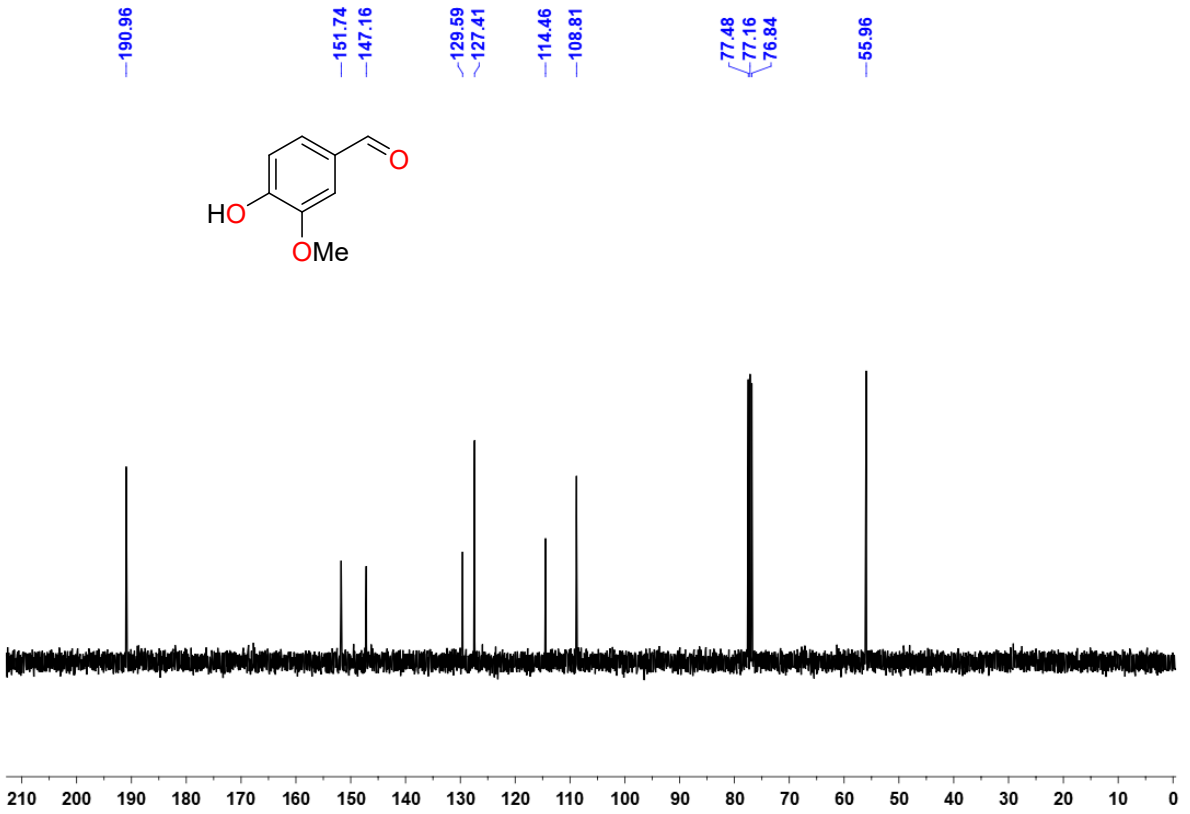

Fig. S28. ^{13}C{^{1}H} NMR spectrum of 4-hydroxy-3-methoxybenzaldehyde (**P$_4$**) in $CDCl_3$ at r.t.

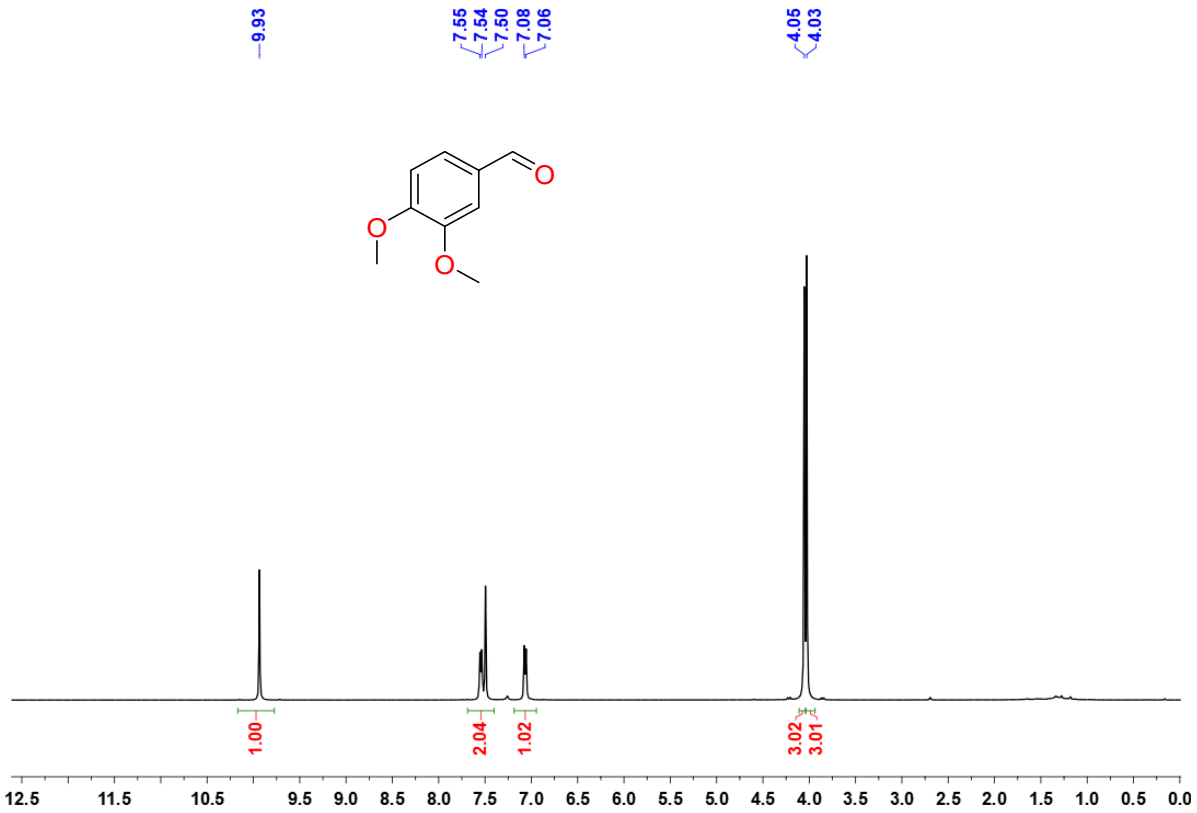

Fig. S29. ^{1}H NMR spectrum of veratraldehyde (**P_5**) in $CDCl_3$ at r.t.

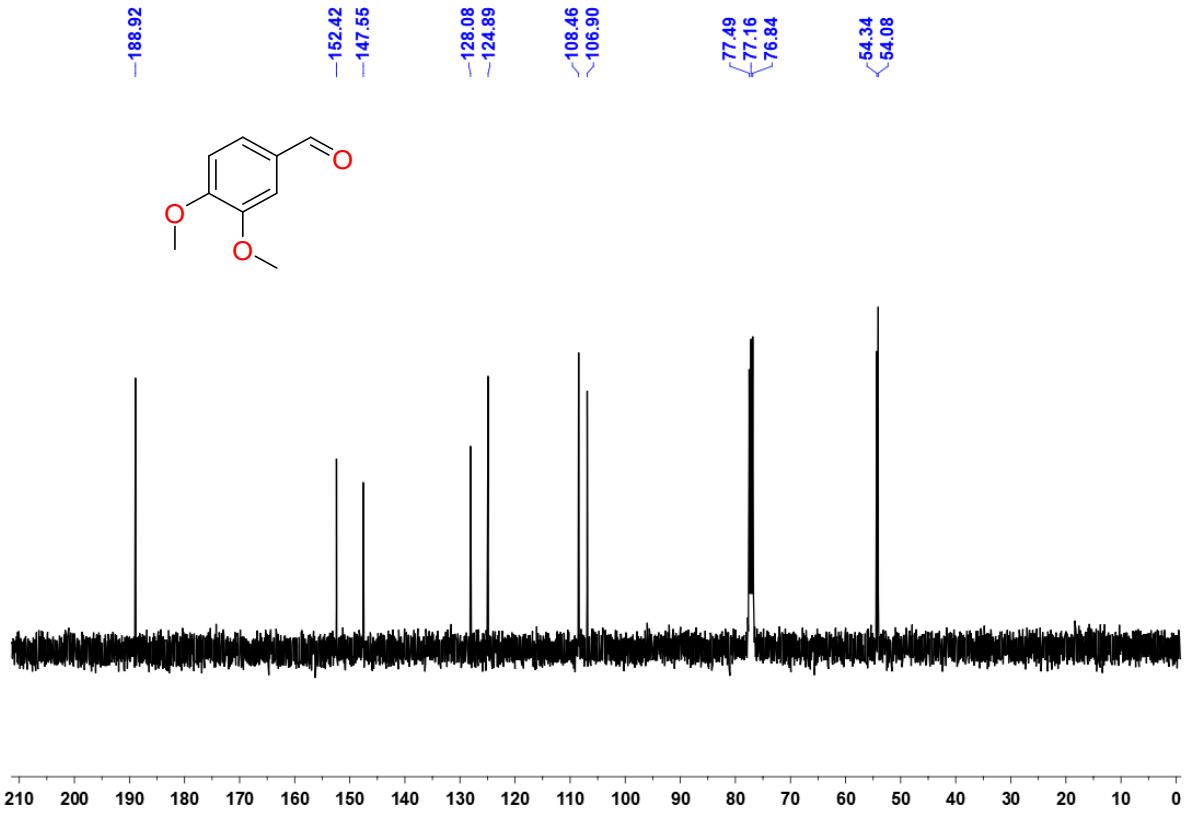

Fig. S30. $^{13}C\{^{1}H\}$ NMR spectrum of veratraldehyde (**P_5**) in $CDCl_3$ at r.t.

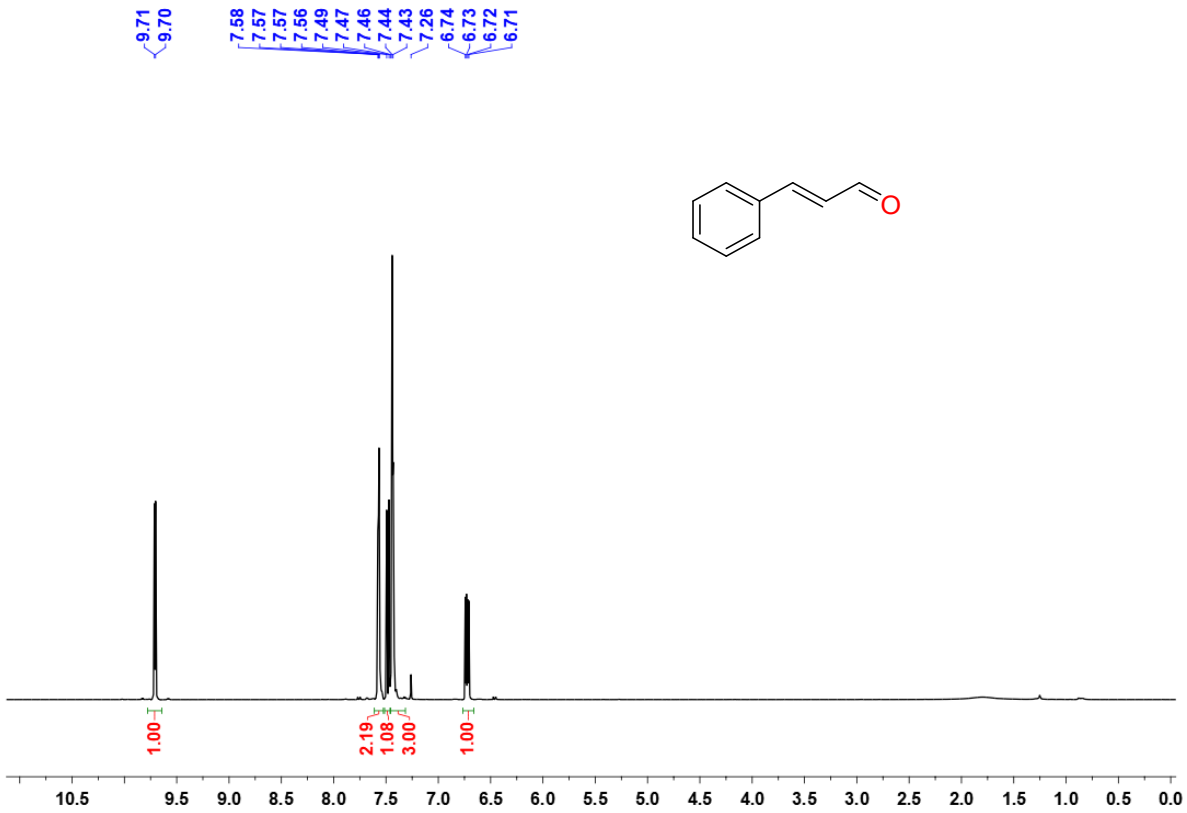

Fig. S31. ^{1}H NMR spectrum of cinnamaldehyde (**P$_6$**) in $CDCl_3$ at r.t.

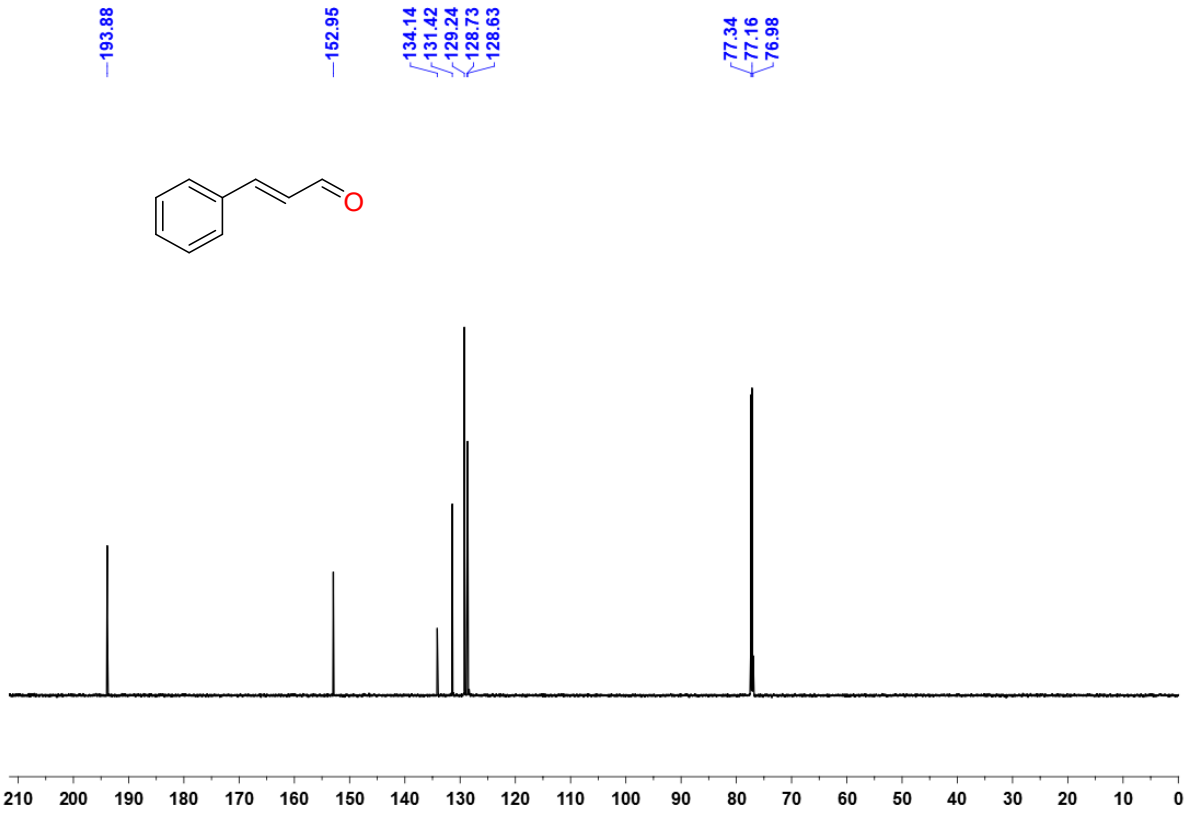

Fig. S32. ^{13}C{^{1}H} NMR spectrum of cinnamaldehyde (**P$_6$**) in $CDCl_3$ at r.t.

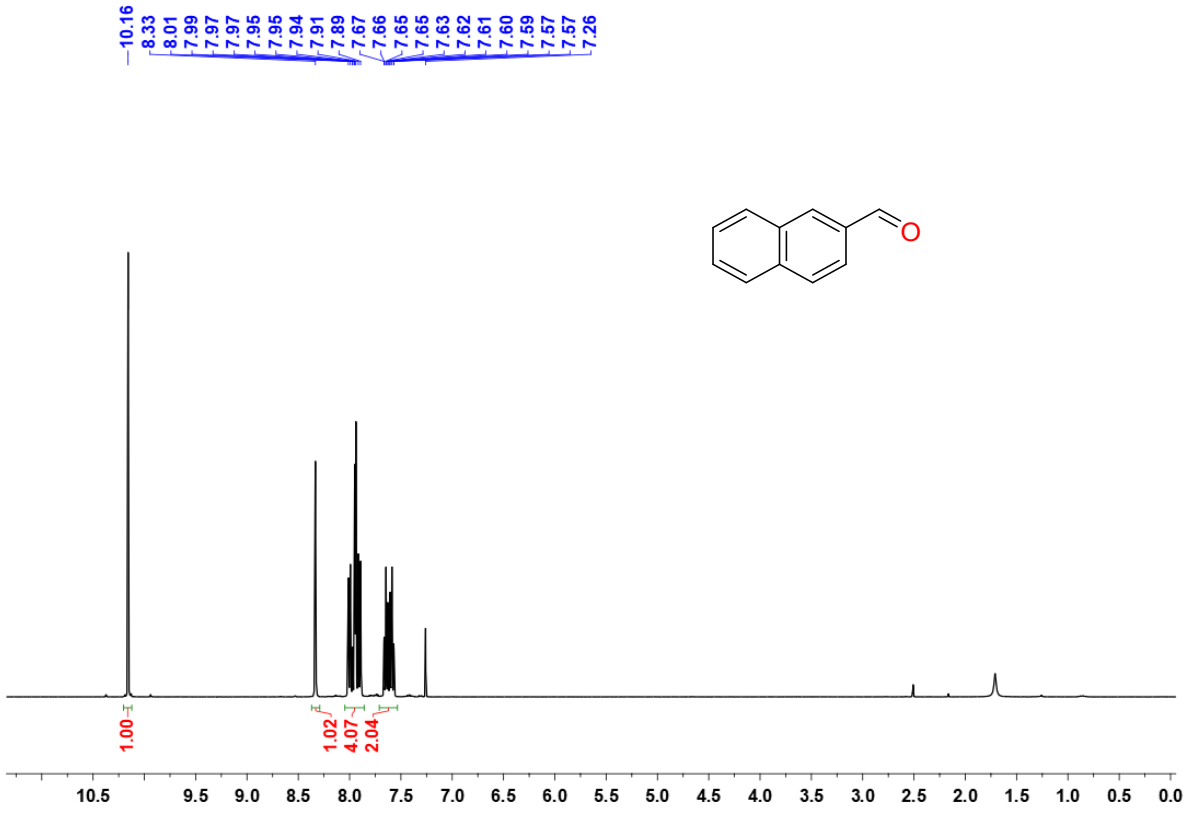

Fig. S33. ^{1}H NMR spectrum of 2-naphthaldehyde (**P**$_7$) in $CDCl_3$ at r.t.

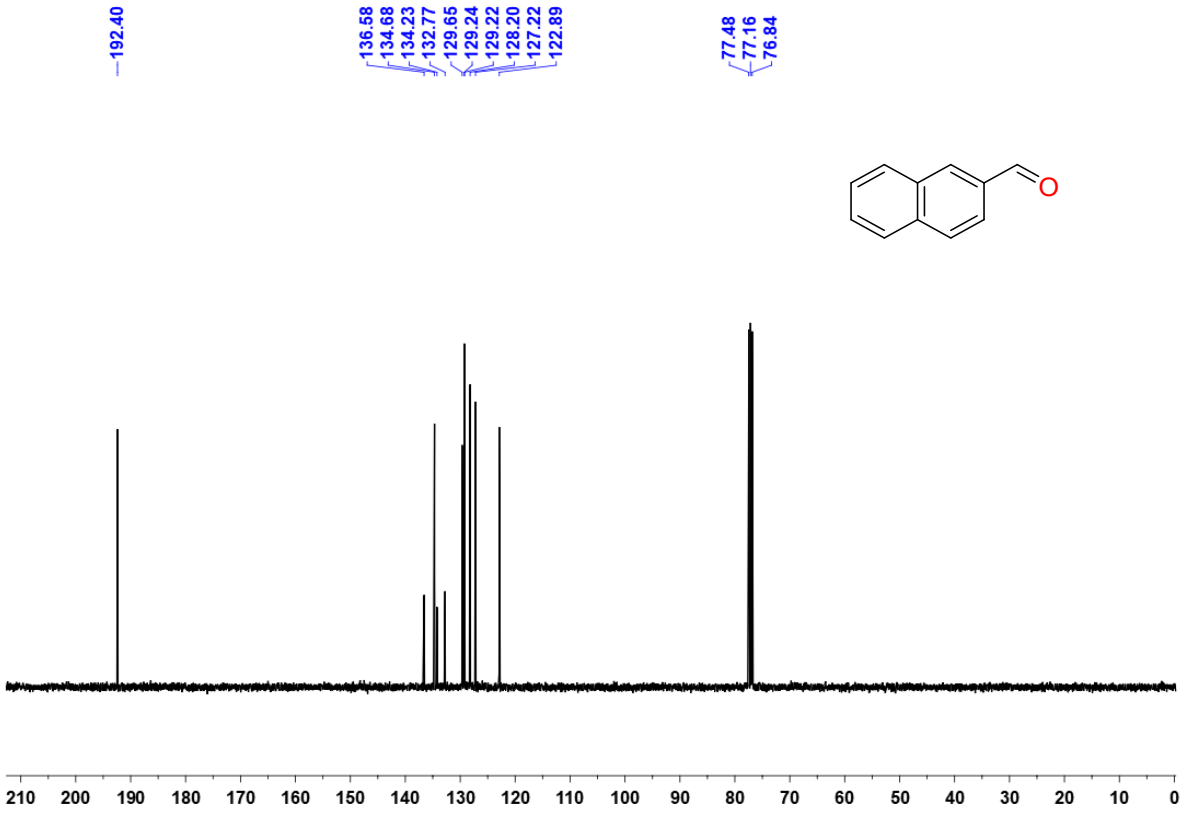

Fig. S34. $^{13}C\{^{1}H\}$ NMR spectrum of 2-naphthaldehyde (**P**$_7$) in $CDCl_3$ at r.t.

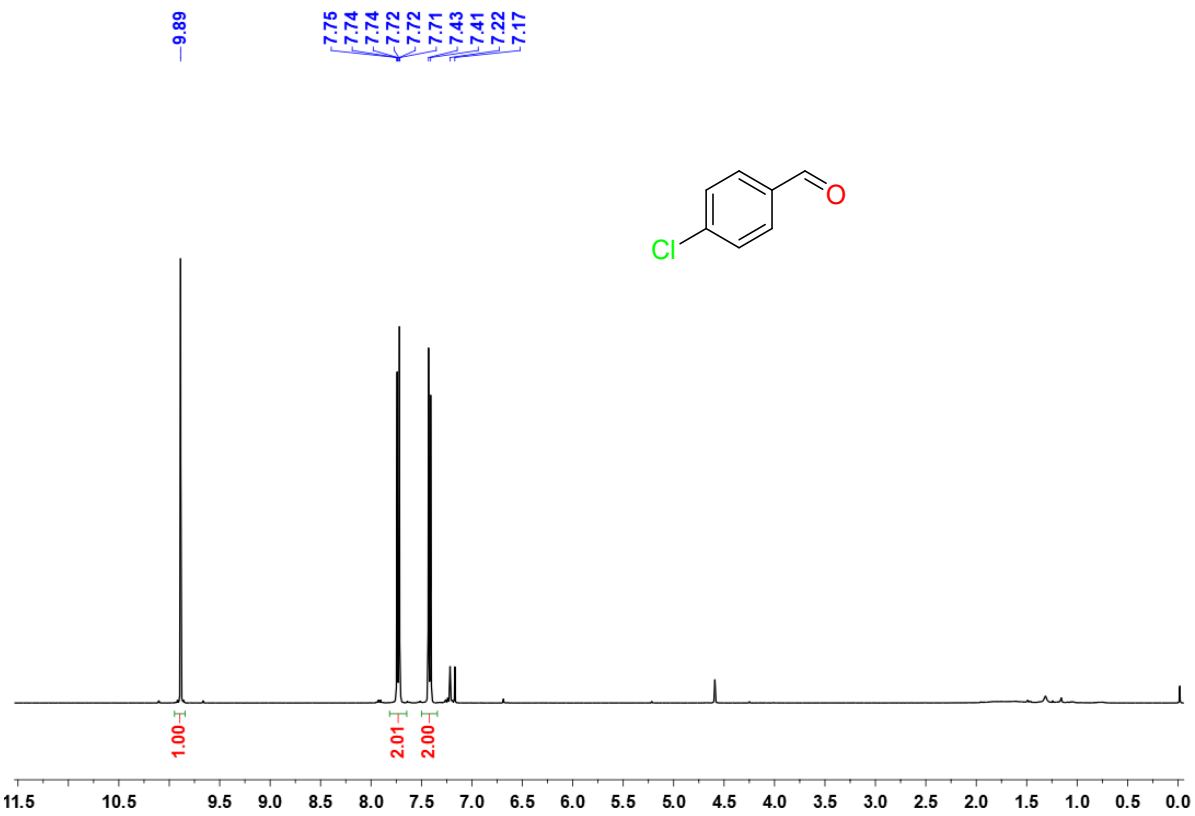

Fig. S35. ^{1}H NMR spectrum of 4-chlorobenzaldehyde (**P_8**) in $CDCl_3$ at r.t.

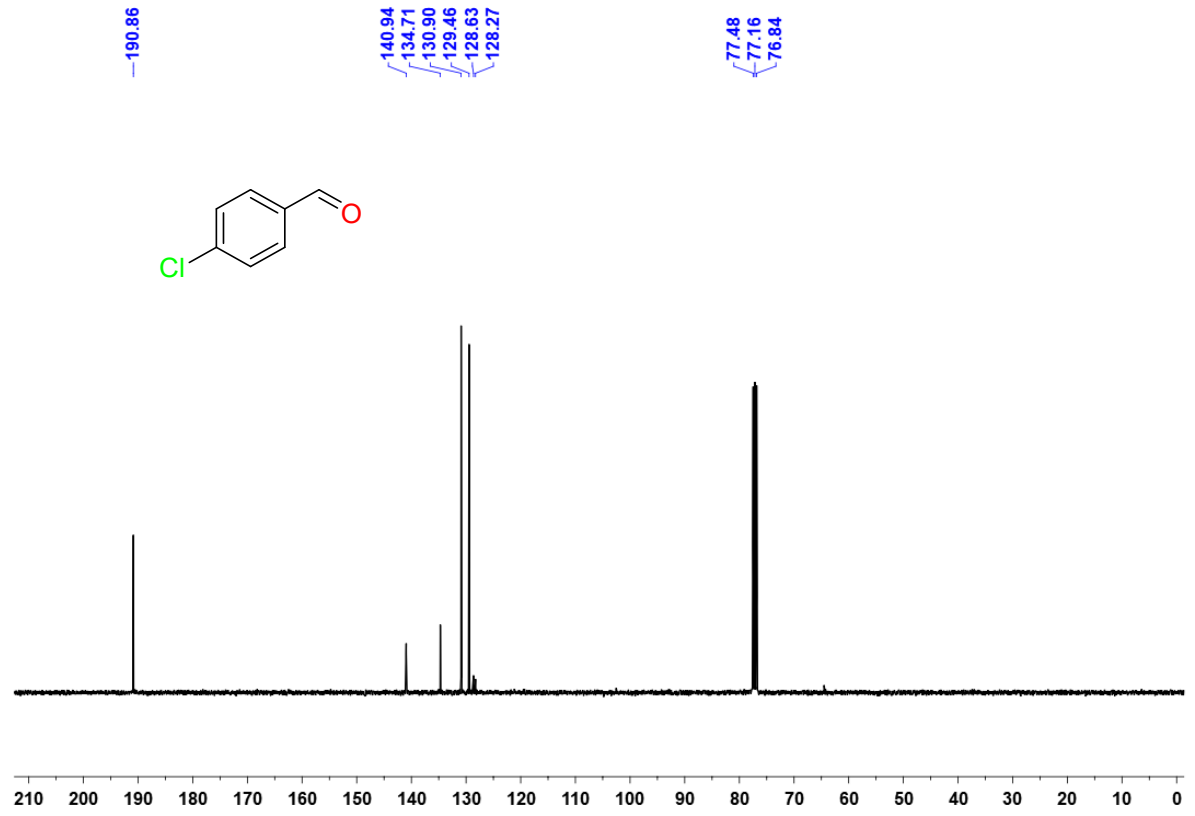

Fig. S36. $^{13}C\{^{1}H\}$ NMR spectrum of 4-chlorobenzaldehyde (**P_8**) in $CDCl_3$ at r.t.

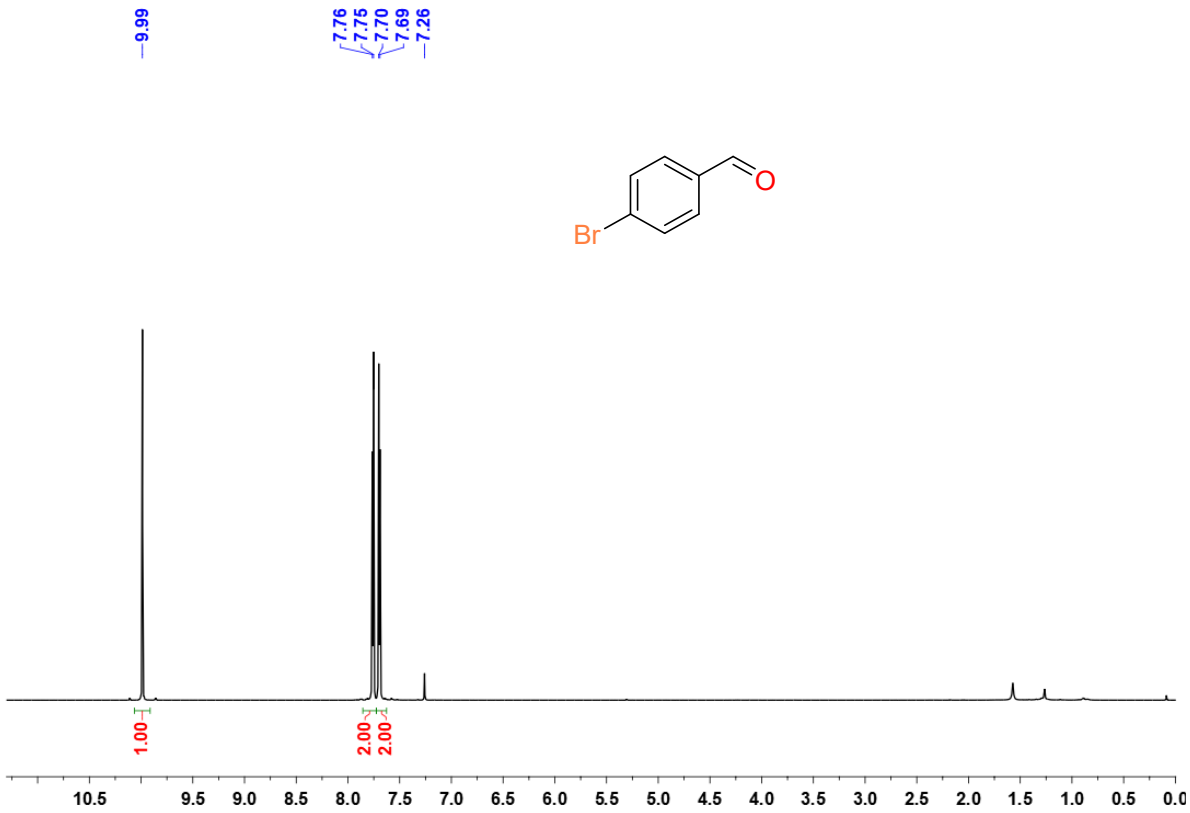

Fig. S37. ^{1}H NMR spectrum of 4-bromobenzaldehyde (**P$_9$**) in $CDCl_3$ at r.t.

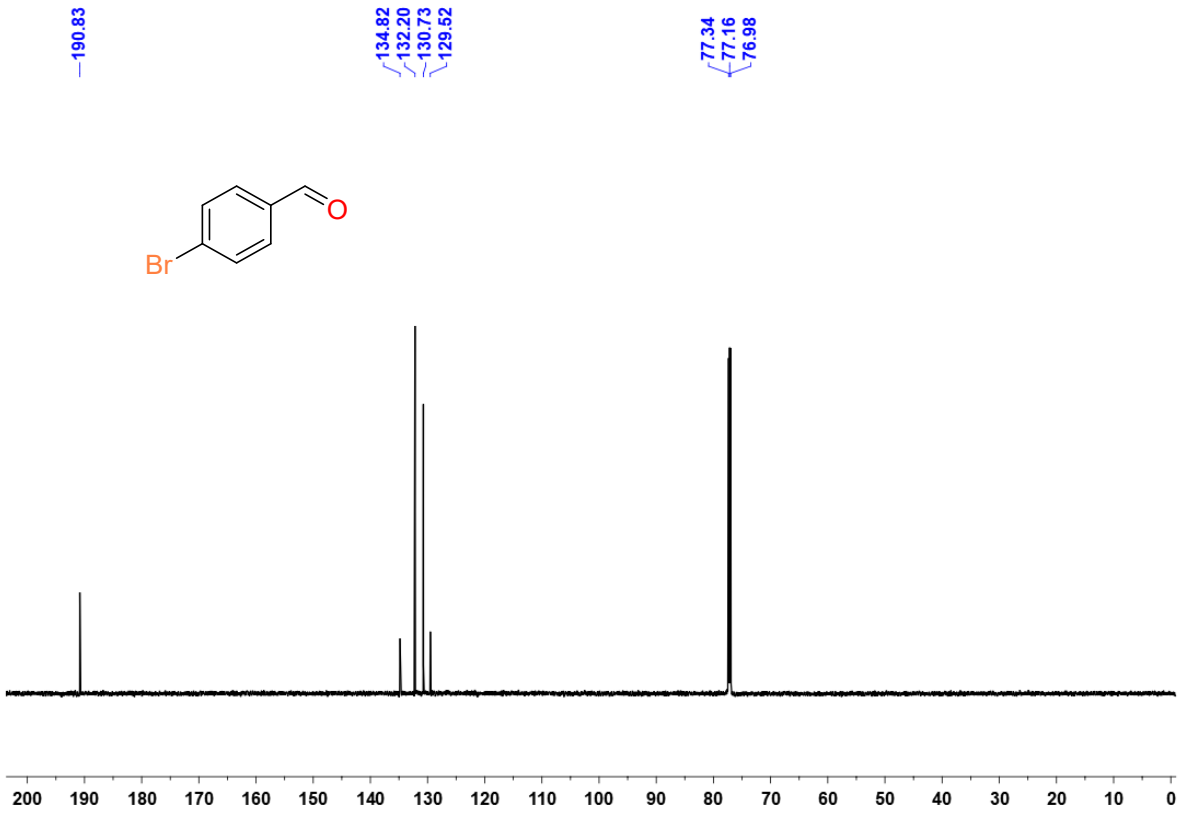

Fig. S38. $^{13}C\{^{1}H\}$ NMR spectrum of 4-bromobenzaldehyde (**P$_9$**) in $CDCl_3$ at r.t.

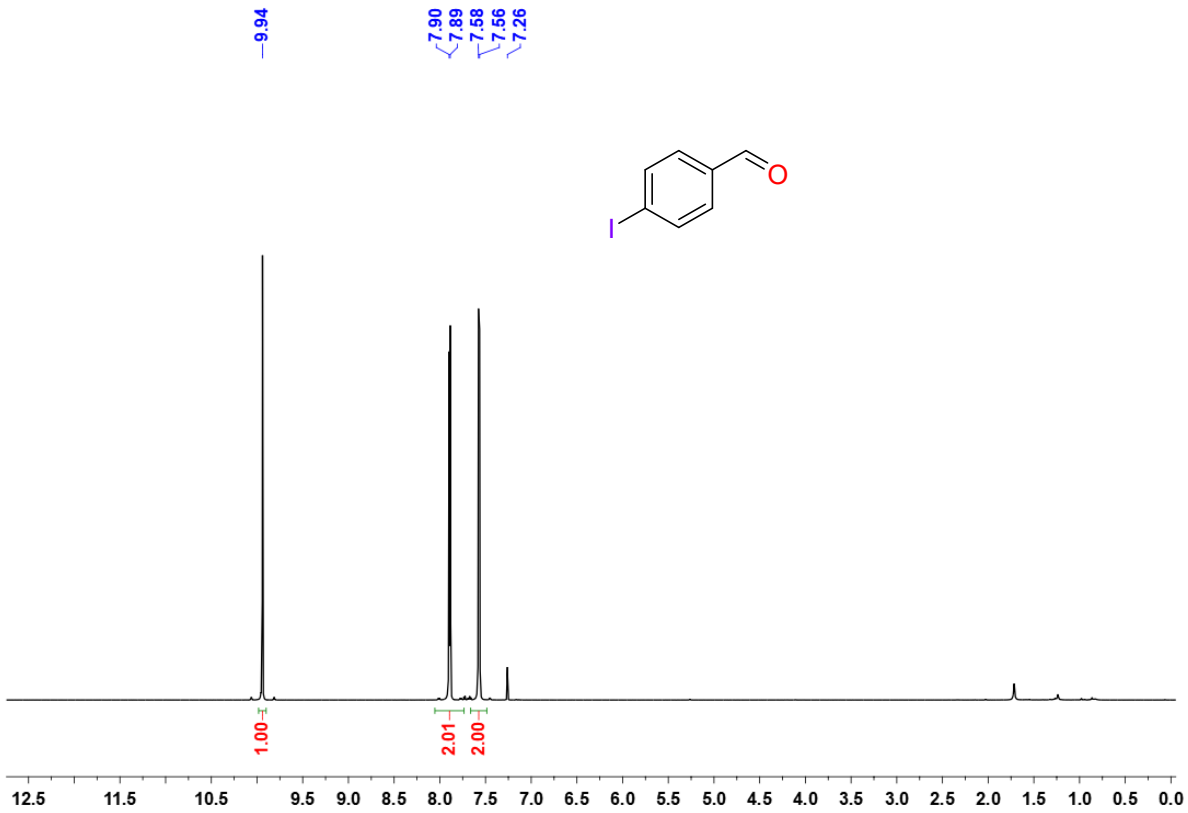

Fig. S39. ^{1}H NMR spectrum of 4-iodobenzaldehyde (**P$_{10}$**) in $CDCl_3$ at r.t.

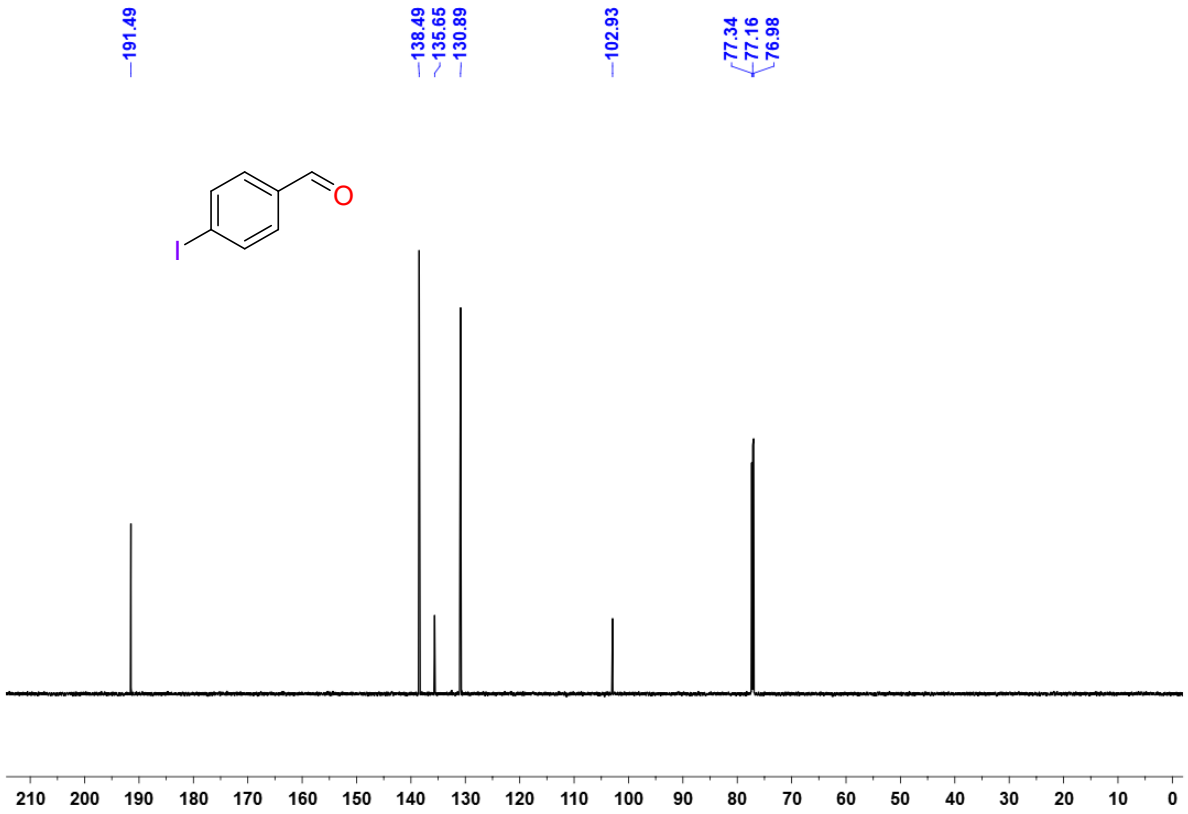

Fig. S40. $^{13}C\{^{1}H\}$ NMR spectrum of 4-iodobenzaldehyde (**P$_{10}$**) in $CDCl_3$ at r.t.

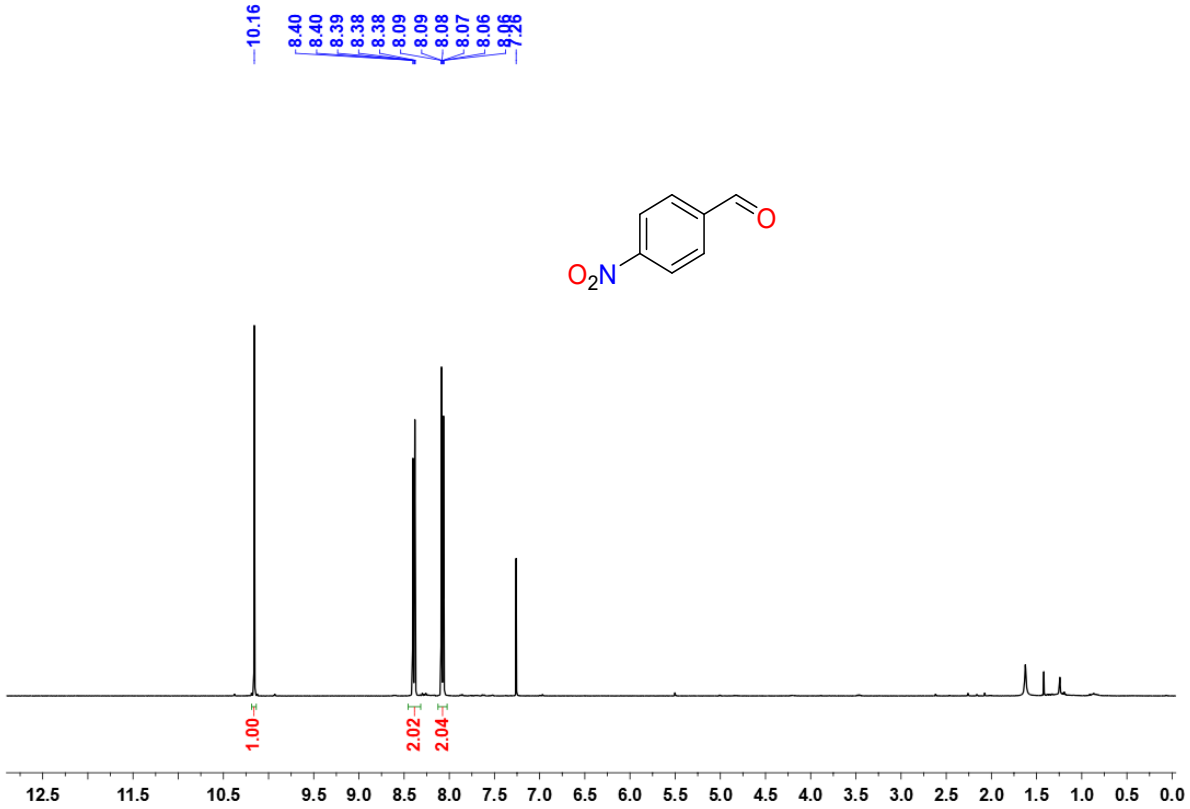

Fig. S41. ^{1}H NMR spectrum of 4-nitrobenzaldehyde (**P$_{11}$**) in $CDCl_3$ at r.t.

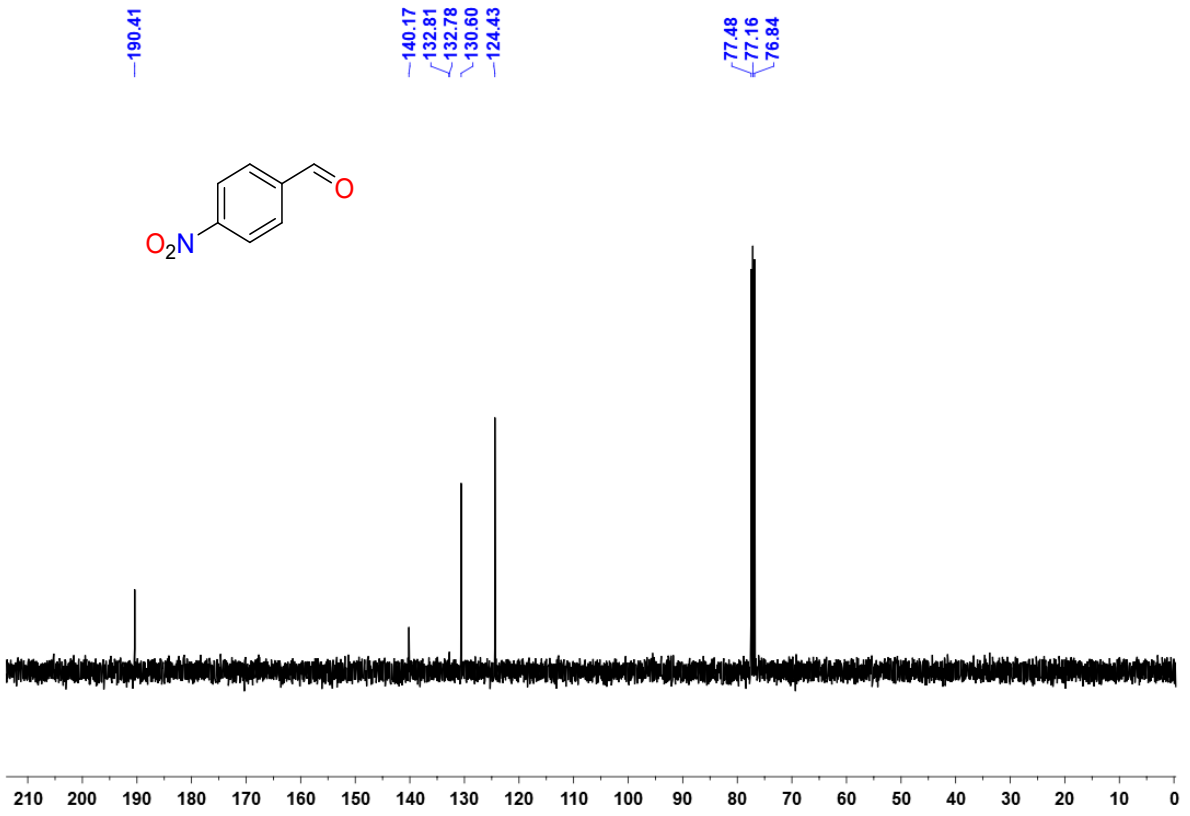

Fig. S42. ^{13}C{^{1}H} NMR spectrum of 4-nitrobenzaldehyde (**P$_{11}$**) in $CDCl_3$ at r.t.

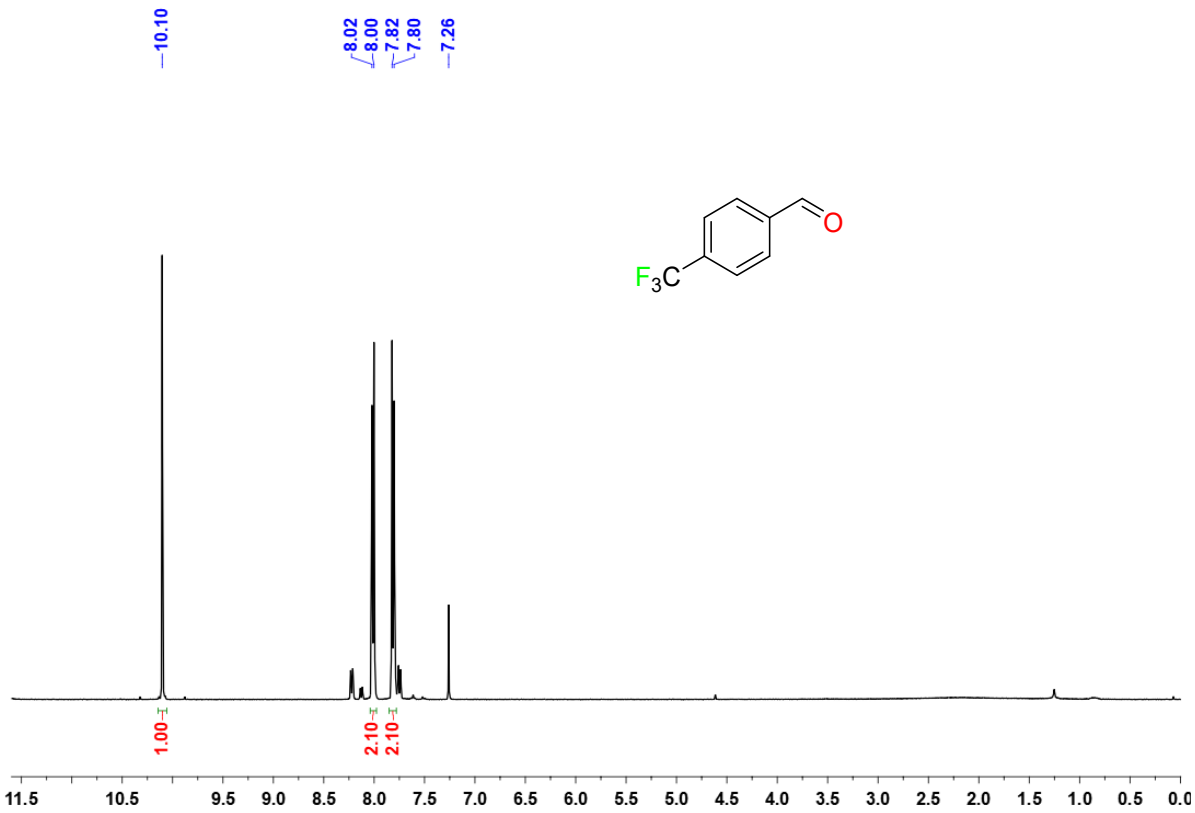

Fig. S43. ^{1}H NMR spectrum of 4-(trifluoromethyl)benzaldehyde (**P$_{12}$**) in $CDCl_3$ at r.t.

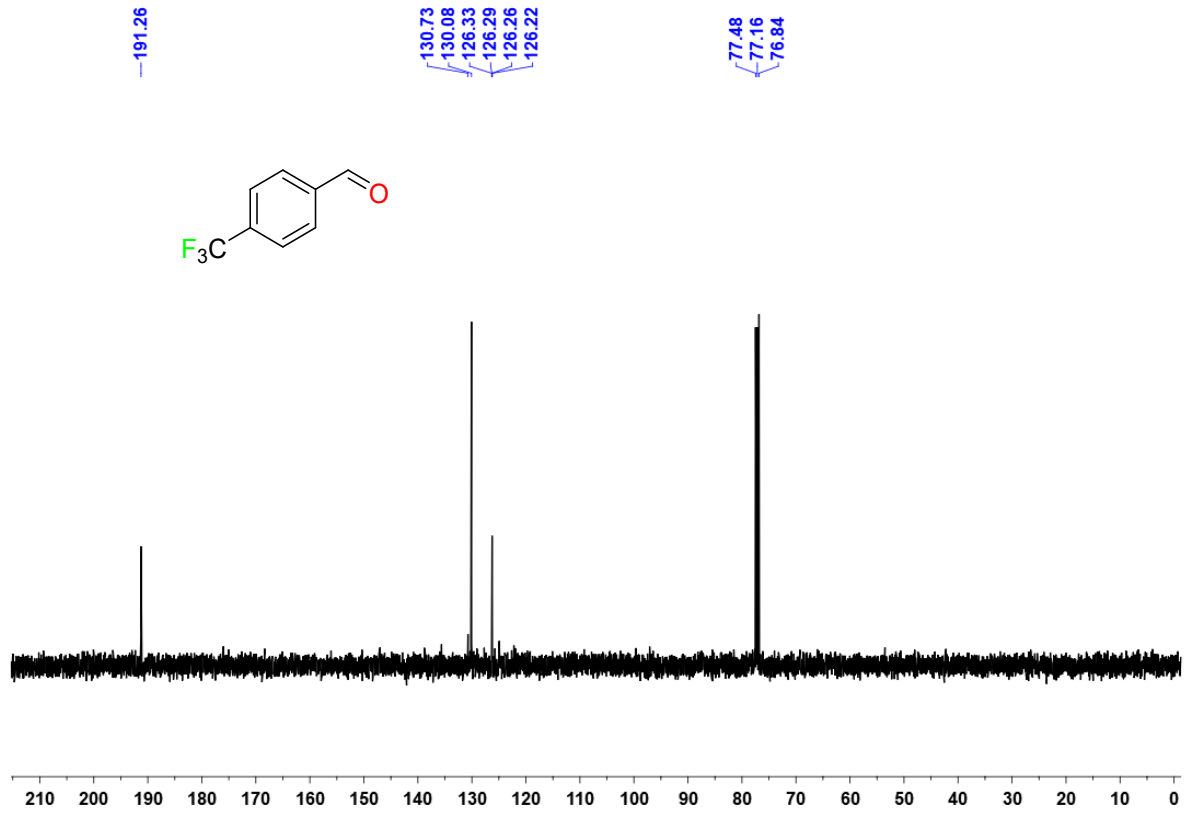

Fig. S44. ^{13}C{^{1}H} NMR spectrum of 4-(trifluoromethyl)benzaldehyde (**P$_{12}$**) in $CDCl_3$ at r.t.

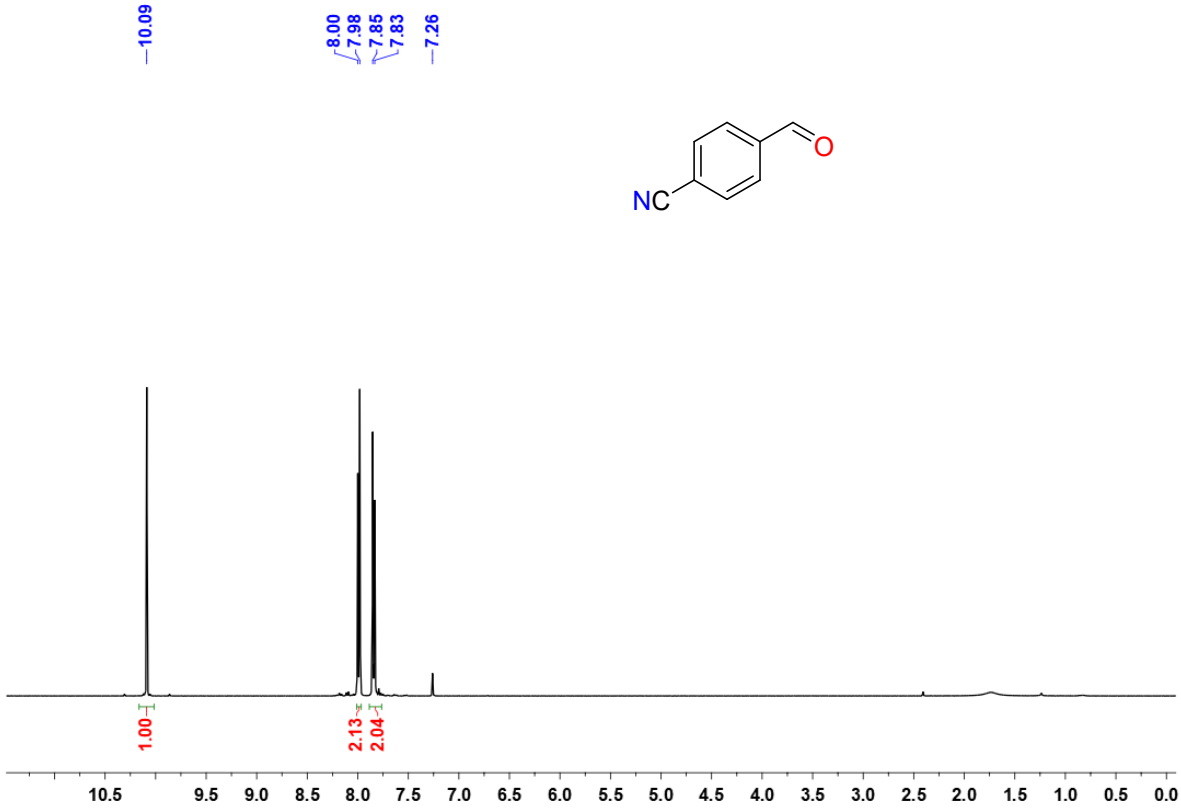

Fig. S45. ^{1}H NMR spectrum of 4-formylbenzonitrile (**P_3**) in $CDCl_3$ at r.t. (* indicates H-grease).

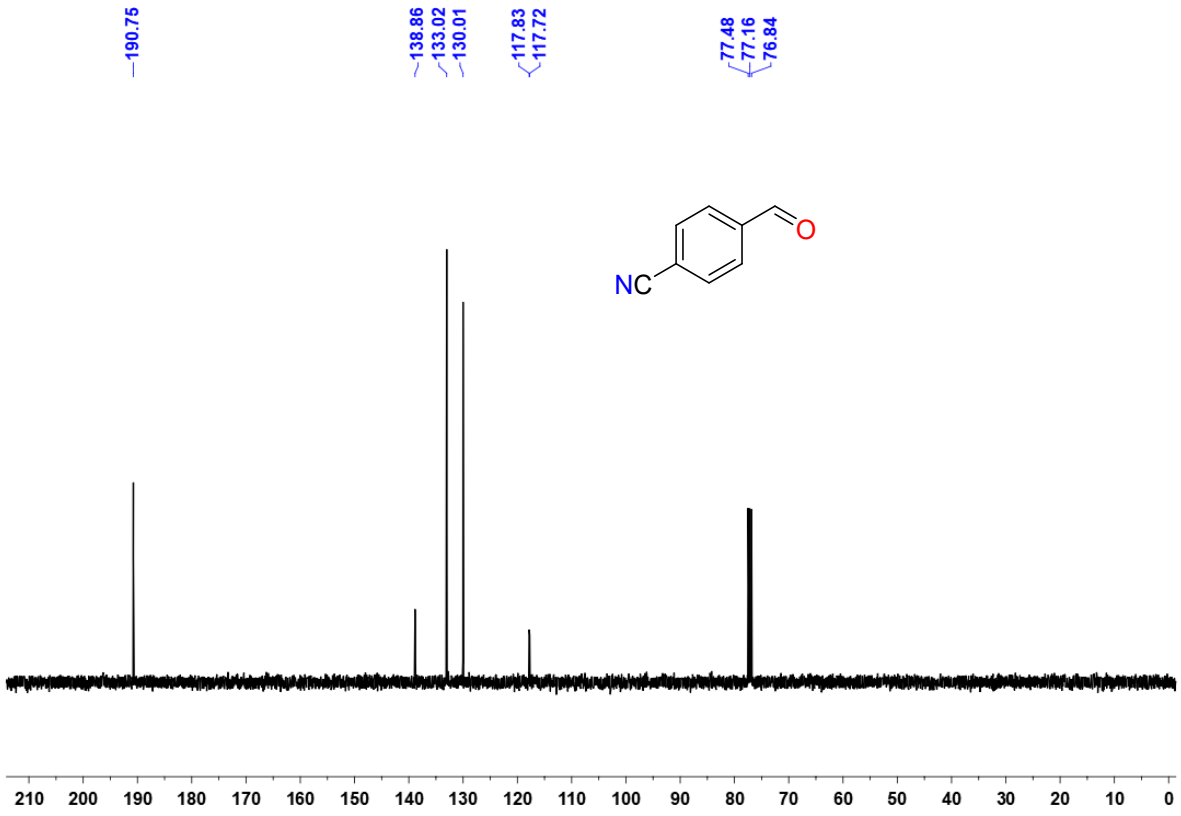

Fig. S46. $^{13}C\{^{1}H\}$ NMR spectrum of 4-formylbenzonitrile (**P_{13}**) in $CDCl_3$ at r.t.

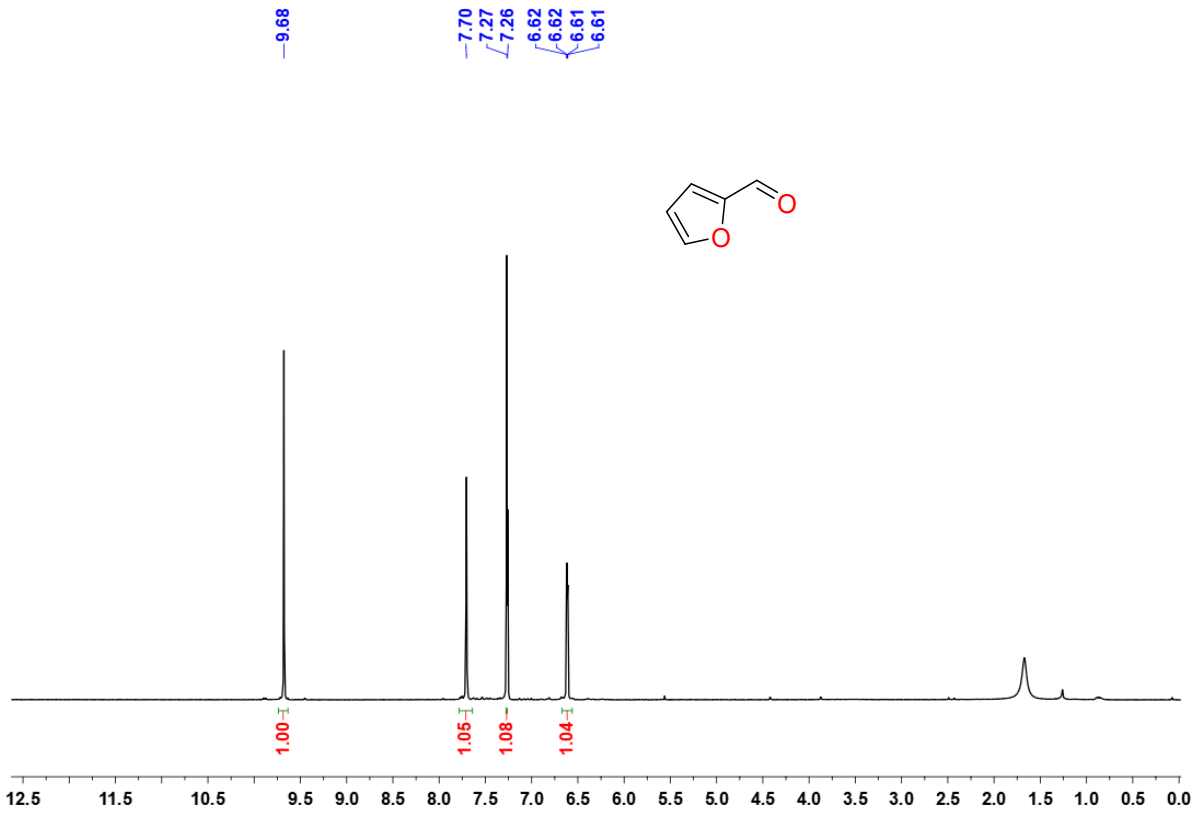

Fig. S47. ^{1}H NMR spectrum of furan-2-carbaldehyde (**P$_{14}$**) in $CDCl_3$ at r.t.

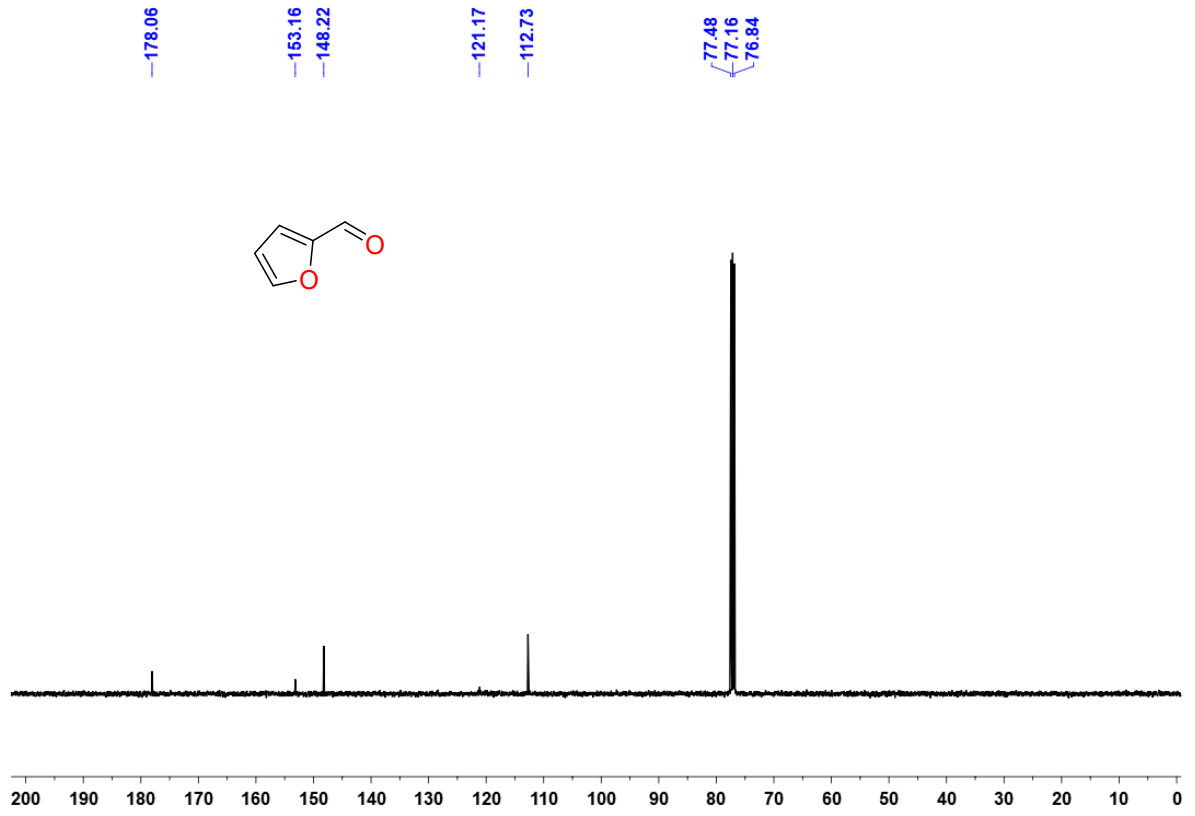

Fig. S48. ^{13}C{^{1}H} NMR spectrum of furan-2-carbaldehyde (**P$_{14}$**) in $CDCl_3$ at r.t.

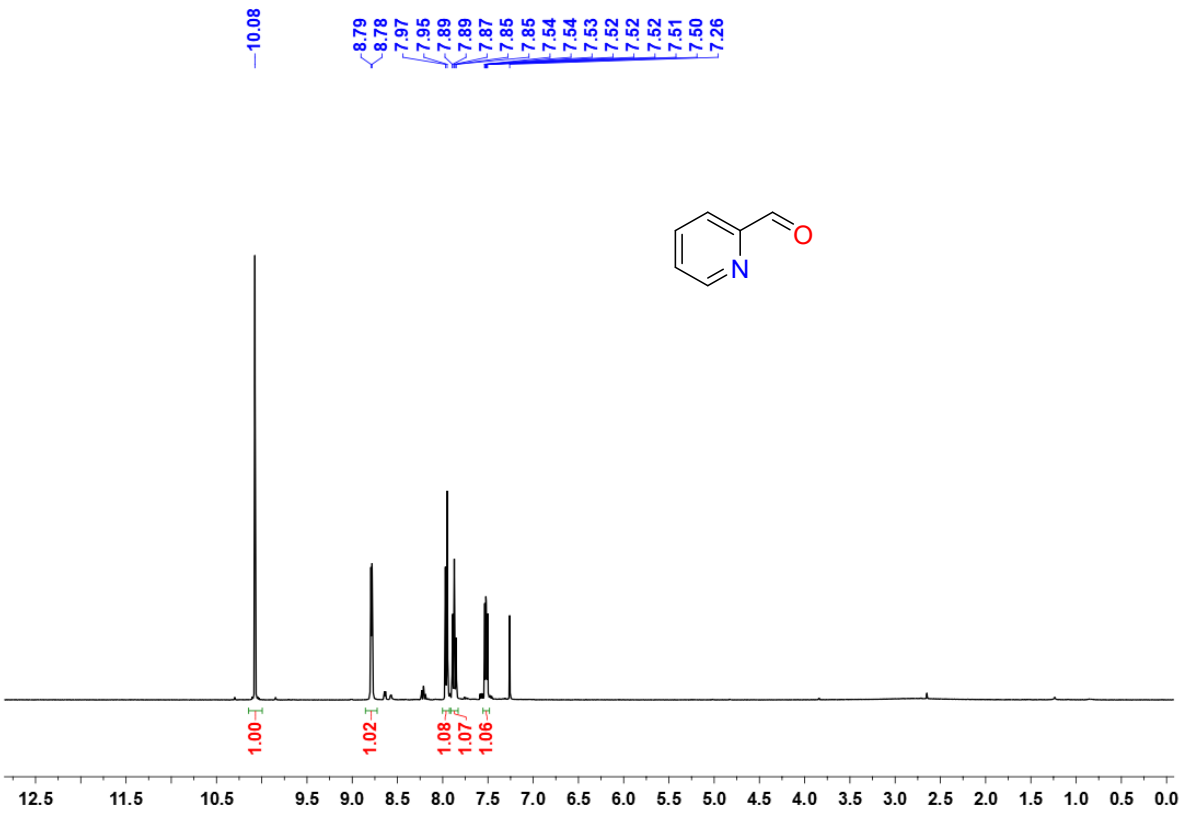

Fig. S49. ^{1}H NMR spectrum of picolinaldehyde (**P$_{15}$**) in $CDCl_3$ at r.t.

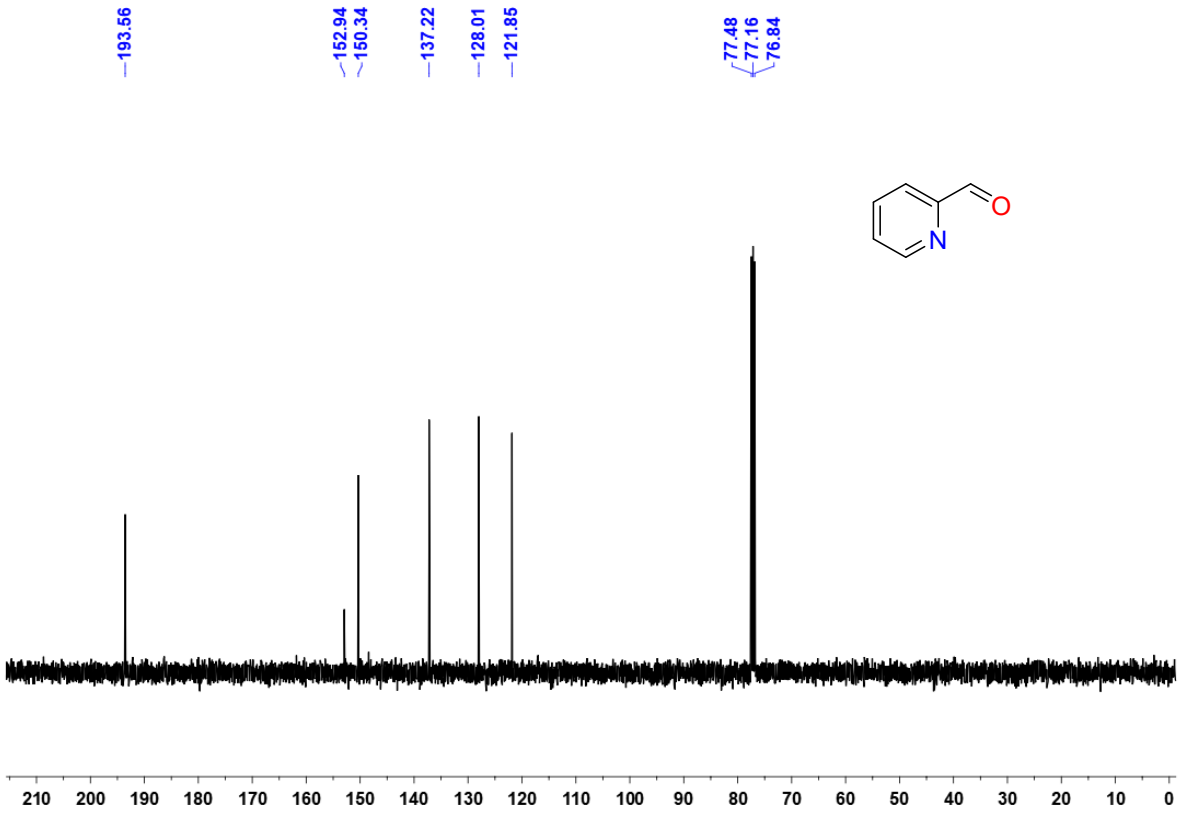

Fig. S50. $^{13}C\{^{1}H\}$ NMR spectrum of picolinaldehyde (**P$_{15}$**) in $CDCl_3$ at r.t.

References

S1 A. De, A. Sengupta, F. Lloret and R. Mukherjee, *Z. Anorg. Allg. Chem*., 2018, **644**, 801–811.

S2 G. A. van Albada, I. Mutikanien, O. Roubeau, U. Turpienen and J. Reedijk, *Inorg. Chim. Acta*, 2002, **331**, 208.

S3 J. Mukherjee, R. Gupta, T. Mallah and R. Mukherjee, *Inorg. Chim. Acta*, 2005, **358**, 2711.

S4 J. Springborg, J. Glerup and I. Sotofte, *Acta Chem. Scand*., 1997, **51**, 832.

S5 A. Escuer, R. Vicente, E. Peñalba, X. Solans and M. Font-Bardía, *Inorg. Chem*., 1996, **35**, 248.

S6 M. Rodríguez, A. Llobet, M. Corbella, P. Müller, M. A. Usón, A. E. Martell and J. Reibenspies, *Dalton Trans*., 2002, 2900.

S7 D. Hu, L. Chen, Z.-Q. Pan, H. Liu, X.-G. Meng and Y. Song, *J. Coord. Chem*., 2008, **61**, 1973.

S8 G. A. van Albada, I. Mutikainen, O. S. Roubeau, U. Turpeinen and J. Reedijk, *Eur. J. Inorg. Chem*., 2000, 2179.

S9 C. Bazzicalupi, A. Bencini, A. Bianchi, V. Fusi, P. Paoletti and B. Valtancoli, *J. Chem. Soc., Chem. Commun*., 1995, 1555.

S10 A. Majumder, C. R. Choudhury, S. Mitra, G. M. Rosair, M. S. El Fallah and J. Ribas, *Chem. Commun*., 2005, 2158

S11 P. Mateus, R. Delgado, F. Lloret, J. Cano, P. Brandao and V. Félix, *Chem. Eur. J*., 2011, **17**, 11193.

S12 S. S. Massoud, F. R. Louka, M. A. Al-Hasan, R. Vicente and F. A. Mautner, *New J. Chem*., 2015, **39**, 5944.

S13 E. A. Malinina, I. K. Kochneva, I. N. Polyakova, V. V. Avdeeva, G. A. Buzanov, N. N. Efimov, E. A. Ugolkova, V. V. Minin and N. T. Kuznetsov, *Inorg. Chim. Acta*, 2018, **479**, 249.